



CONTENTS

1 From the Director

SCIENCE HIGHLIGHTS:

2 SMA Imaging of CO in the Hypervolatile-Rich Comet C/2016 R2 (PanSTARRS)

5 Evolution and Kinematics of Protostellar Envelopes in the Perseus Molecular Cloud

9 Core Mass Function of a Single Giant Molecular Cloud Complex with ~10,000 Cores

TECHNICAL HIGHLIGHTS:

12 A Look at the wSMA Receiver Cartridge

15 RTDC News

OTHER NEWS

18 2022 Submillimeter Array Interferometry School

19 Staff Changes in Hilo

John Maute Retires

SMA Postdoctoral Fellows

20 Call for Proposals

21 Proposal Statistics

Track Allocations

22 Top-Ranked Proposals

23 All SAO Proposals

25 Recent Publications

FROM THE DIRECTOR

Dear SMA Newsletter readers,

As many of you know, the SMA has continued to operate and make scientific observations advancing a wide range of astrophysics during the past two years of pandemic, albeit with somewhat reduced effectiveness due to covid restrictions. I'm happy to note that SMA staff in Cambridge (MA), along with our other colleagues at the Center for Astrophysics, are now fully on the road to returning to work on-site. Only last week I needed to chat with another staff member—following our remote work habit I sent a Slack message 'Do you have time for a brief chat?'. An almost instant video call in reply: 'Oh, you're in the office? So am I, I'll come over'. Collectively we have learned a lot during this period of forced separation, but those casual conversations in the hallways, ideas exchanged in person, and memories jogged as people pass in the corridor have been missed.

Coupled with a full return to on-site work, the arrival of new CfA Director Lisa Kewley, and ongoing progress towards the wSMA, I am optimistic that with renewed energy and sense of purpose we are on the road to being more productive than ever!

Best wishes,

Raymond Blundell

SMA IMAGING OF CO IN THE HYPERVOLATILE-RICH COMET C/2016 R2 (PANSTARRS)

M. A. CORDINER,^{1,2} C. QI,³ Y.-J. KUAN,^{4,5} E. GARCIA-BERRIOS,^{1,2} F. LIQUE,⁶ M. ZOŁTOWSKI,^{6,7} M. DE VAL-BORRO,^{1,2} W.-H. IP,⁸ I. M. COULSON,⁹ S. MAIRS,⁹ N. X. ROTH,^{1,2} S. B. CHARNLEY,¹ S. N. MILAM,¹ W.-L. TSENG,⁴ AND Y.-L. CHUANG⁴

Comets are composed of ice, dust and debris accreted during the epoch of planet formation. Having spent most of their lives frozen, at large distances from the Sun, cometary nuclei contain some of our Solar System's most pristine (thermally unprocessed) material. From studies of their gaseous atmospheres (comae), the properties of the nucleus can be inferred, thereby providing unique insights into the conditions prevalent at the dawn of the Solar System.

The long-period comet C/2016 R2 (PanSTARRS) was discovered in August 2016, and reached perihelion in May 2018. Optical spectroscopy revealed a highly unusual spectrum, dom-

inated by CO⁺ emission, in addition to a rare detection of N₂⁺ (Cochran & McKay 2018). Both CO and N₂ sublimate at low temperatures compared to other cometary ices (e.g. Womack et al. 2017), and are therefore considered 'hypervolatile'. Their presence in very high abundances implies that C/2016 R2 formed very cold, and was maintained at temperatures ≤ 20 K for the duration of its lifetime. Spectrally and spatially resolved mm-wave spectroscopy of C/2016 R2 provides the opportunity to investigate the nature of outgassing from this exceptionally rare class of comet.

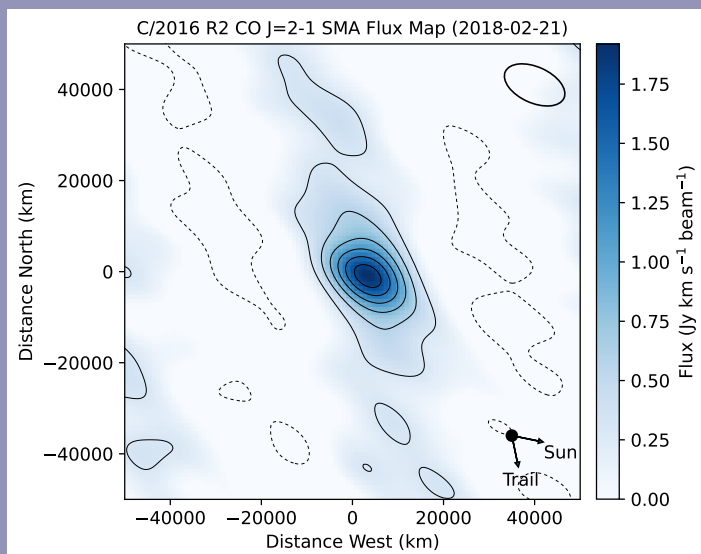


Figure 1: Spectrally integrated CO $J = 2 - 1$ emission map for comet C/2016 R2, obtained using the SMA on 2018-02-21. The FWHM (and orientation) of the elliptical Gaussian restoring beam is indicated upper-right, and the sky-projected solar and orbital trail vectors are shown lower right. Contours are in units of 3σ and the axes are aligned with the equatorial (RA/dec.) grid, with the origin at the SMA phase tracking center. Negative contours are shown in dashed lines.

¹Astrochemistry Laboratory, NASA Goddard Space Flight Center; ²Department of Physics, Catholic University of America; ³Center for Astrophysics | Harvard & Smithsonian; ⁴National Taiwan Normal University; ⁵Institute of Astronomy and Astrophysics, Academia Sinica; ⁶Université de Rennes; ⁷CNRS-Université du Havre; ⁸Graduate Institute of Space Science, National Central University, Taiwan.; ⁹East Asian Observatory

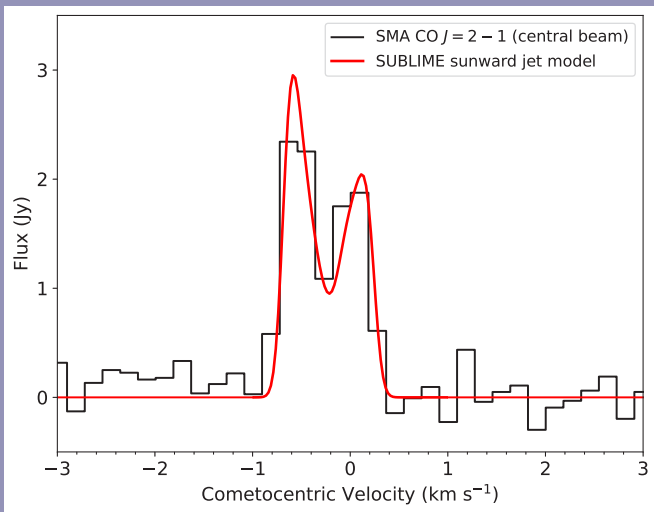


Figure 2: CO $J = 2 - 1$ spectrum observed with the SMA (extracted at the CO emission peak), with best-fitting 2-component SUBLIME model overlaid using a red curve.

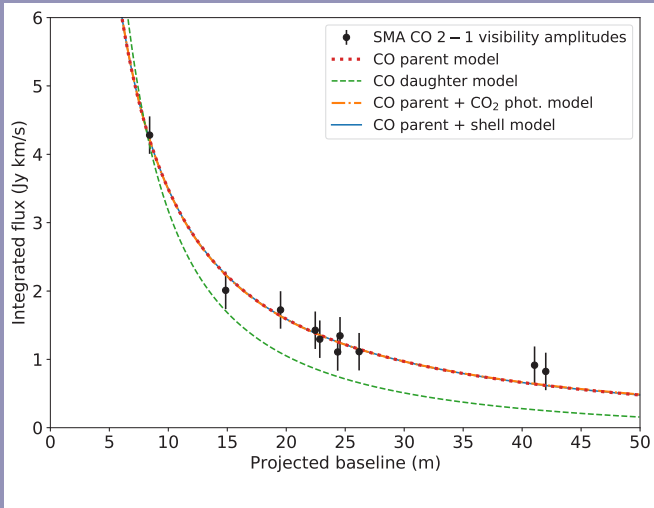


Figure 3: CO $J = 2 - 1$ visibility amplitudes vs. baseline length for C/2016 R2 observed using the SMA, including 1σ statistical error bars. Model visibility curves are overlaid for four different CO distributions. The CO parent, parent + CO₂ photolysis, and parent + shell model curves all lie on top of each other, whereas the CO daughter curve differs significantly, under-fitting the observations at large baseline (small angular scales).

During 2018 January and February, we undertook a program of single-dish and interferometric observations of comet C/2016 R2 using the James Clerk Maxwell Telescope (JCMT) and Submillimeter Array (SMA) (Cordiner et al. 2022). The resulting (spectral-spatial-temporal) dataset was analyzed using a new, time-dependent, three dimensional radiative transfer code (called SUBLIME), which includes excitation via collisions with CO and electrons, as well as radiative processes.

SMA observations were made on 2018-02-21, when the comet was at a heliocentric distance $r_H = 2.7$ au and Geocentric distance $\Delta = 2.5$ au. The two SMA receivers were both tuned to 1.3 mm to cover the CO $J = 2 - 1$ transition at 230.538 GHz. With five antennas in the subcompact (SUB) configuration, the spatial resolution was $\approx 4.4'' \times 7.7''$ at 230 GHz.

The CO $J = 2 - 1$ intensity map is shown in Figure 1, integrated over the velocity range of the detected emission. The coma shows an extended morphology in an approximately N-S direction, and is less well resolved in the E-W direction, where significant large-scale flux appears to have been resolved out by the interferometer, resulting in negative side lobes on either side of the comet.

As a result of near-spherical expansion, cometary comae span an extremely broad range of densities over a short distance. Consequently, the interpretation of their rotational spectra requires detailed, non-LTE radiative transfer modeling. We used the SUBLIME (SUBLimating gases in LIME) code (Cordiner et al. 2022; Brinch & Hogerheijde 2010) to simulate the CO emission line in three dimensions. Our model employs two CO outflow components emanating from the nucleus: C₁ and C₂, corresponding to solid angle regions (Ω_1, Ω_2) with independent production rates (Q_1, Q_2) and outflow velocities (v_1, v_2). Component C₁ corresponds to a conical jet with its axis oriented along the comet-sun vector, and C₂ represents the remaining (ambient) coma.

An initial model fit was performed to the CO $J = 2 - 1$ spectral line profile extracted at the emission peak of the CO map (Figure 1). The parameters Q_1, Q_2, v_1, v_2 , and the C₁ cone half-opening angle (θ) were free to vary, while the kinetic temperature was fixed at the value of 18.7 K derived from the JCMT CO $J = 3 - 2$ and $2 - 1$ data (Cordiner et al. 2022). The best-fitting spectral line model is shown in Figure 2, and corresponds to $v_1 = 0.64 \pm 0.02$ km s⁻¹, $v_2 = 0.20 \pm 0.02$ km s⁻¹, and $\theta = 74^\circ \pm 7^\circ$.

From this initial 'CO parent' model, additional models were constructed assuming (1) CO as solely a daughter species, with parent scale length $\Gamma_p = 7.3 \times 10^{-5}$ s⁻¹ (derived from the JCMT data of Cordiner et al. 2022), (2) CO as a parent species with additional outer-coma CO source from CO₂ photolysis, and (3) CO as a parent with an additional, extended CO shell at a radius $r_s = 1.2 \times 10^5$ km, with a density-enhancement factor $f = 1.8$. The resulting 3D model images were integrated in the spectral domain then multiplied by the (FWHM = 55'') SMA primary beam pattern before sampling in the Fourier domain using the `vis_sample` code (Loomis et al. 2018). A power-law curve (ax^b) was fit through each set of model results, (with x the baseline length, and a and b free parameters), and plotted along with the observed, time-averaged visibility amplitudes in Figure 3. For clarity, the model visibility curves were scaled vertically in order to pass through the

shortest-baseline point. The total CO production rate of the best-fitting (scaled) parent model is $Q(\text{CO}) = (6.7 \pm 0.9) \times 10^{28} \text{ s}^{-1}$ (including a 10% amplitude calibration error in addition to the statistical error).

Three of the model curves (parent, parent + CO₂ photolysis, and parent + extended shell) all represent an equally good fit to the observations, falling precisely on top of each other in **Figure 3**. This implies that the SMA would have been blind to the additional CO component observed at large radii in the JCMT maps of Cordiner et al. (2022) — i.e. the extended CO component was smooth enough on large angular scales not to be detected on even the shortest SMA baselines. In contrast, the CO daughter model does not fit the observed visibilities well, with insufficient flux on small angular scales (long baselines). Consequently, the SMA observations rule out the possibility of CO being solely a daughter species in this comet, although significant production at large radii (for example, from CO₂ photolysis) is still possible.

The CO production rate measured using the SMA confirms C/2016 R2 as having among the highest CO production rates ever observed in a comet — only a factor of 4 less than C/1995 O1 (Hale Bopp) at similar heliocentric distances. Our 3D spectral line modeling demonstrates a strong preference for CO outgassing from the sunward-facing hemisphere of the comet, with a production rate ratio (per unit solid angle) of 9.2 ± 1.5 between outflow components C₁ and C₂. The asymmetric, blueshifted CO line profile of C/2016 R2 is similar to that of the large Centaur 29P/SW 1 (Festou et al. 2001; Gunnarsson et al. 2002), as well as to the CO line profile observed in C/1995 O1 at $r_H \approx 8$ au (Gunnarsson et al. 2003). Our interpretation of the line shape in terms of enhanced CO production and outflow velocity on the sunward side of the nucleus is consistent with Gunnarsson et al. (2008)'s analysis of the 29P coma.

REFERENCES

- Biver, N., Bockelée-Morvan, D., Paubert, G., et al. 2018, A&A, 619, A127, doi: 10.1051/0004-6361/201833449
- Brinch, C., & Hogerheijde, M. R. 2010, A&A, 523, A25, doi: 10.1051/0004-6361/201015333
- Cochran, A. L., & McKay, A. J. 2018, ApJL, 854, L10 doi: 10.3847/2041-8213/aaab57
- Cordiner, M. A., Coulson, I. M., Garcia-Berrios, E., et al. 2022, ApJ, 929, 38, doi: 10.3847/1538-4357/ac5893
- Festou, M. C., Gunnarsson, M., Rickman, H., Winnberg, A., & Tancredi, G. 2001, Icarus, 150, 140, doi: 10.1006/icar.2000.6553
- Gunnarsson, M., Bockelée-Morvan, D., Biver, N., Crovisier, J., & Rickman, H. 2008, A&A, 484, 537, doi: 10.1051/0004-6361:20078069
- Gunnarsson, M., Rickman, H., Festou, M. C., Winnberg, A., & Tancredi, G. 2002, Icarus, 157, 309, doi: 10.1006/icar.2002.6839
- Gunnarsson, M., Bockelée-Morvan, D., Winnberg, A., et al. 2003, A&A, 402, 383, doi: 10.1051/0004-6361:20030178
- Loomis, R. A., Öberg, K. I., Andrews, S. M., et al. 2018, AJ, 155, 182, doi: 10.3847/1538-3881/aab604
- McKay, A. J., DiSanti, M. A., Kelley, M. S. P., et al. 2019, AJ, 158, 128, doi: 10.3847/1538-3881/ab32e4
- Price, E. M., Cleaves, L. I., Bodewits, D., & Öberg, K. I. 2021, ApJ, 913, 9, doi: 10.3847/1538-4357/abf041
- Womack, M., Sarid, G., & Wierzbach, K. 2017, PASP, 129, 031001, doi: 10.1088/1538-3873/129/973/031001

Using the $Q(\text{H}_2\text{O})$ value from McKay et al. (2019), the CO/H₂O ratio in C/2016 R2 is ~37 times larger than seen in any comet to-date (including the distant Centaur 29P, for which the surface temperature is too cold for H₂O to sublimate). When considering this result, along with peculiar abundances of HCN, CH₄, CH₃OH and H₂CO (Biver et al. 2018; McKay et al. 2019), our SMA results confirm that C/2016 R2 is among the most unusual and CO-rich comets ever observed. Such a strongly enhanced CO abundance implies a dramatically different formation (and/or evolutionary history) for this comet, compared with the general cometary population in our Solar system. Biver et al. (2018) suggested that C/2016 R2 could be a CO-rich fragment of a thermally-differentiated Kuiper Belt object, whereas McKay et al. (2019) considered a possible explanation as an interstellar (alien) comet captured from a different star system. Indeed, strongly enhanced CO ice abundances may arise under certain circumstances as a result of pebble drift and gas diffusion during comet formation in protoplanetary disks (Price et al. 2021). Alternatively, Cordiner et al. (2022) raised the possibility of an insulating surface crust on the comet, which may have hindered the outgassing of H₂O, while still allowing the hypervolatile CO and associated (trapped) volatiles to sublimate.

ACKNOWLEDGMENTS

This work was supported by the National Science Foundation under Grant No. AST-2009253. The work of SNM, NXR, MAC, EGB and SBC was also supported by NASA's Planetary Science Division Internal Scientist Funding Program through the Fundamental Laboratory Research work package (FLaRe). The Submillimeter Array is a joint project between the Smithsonian Astrophysical Observatory and the Academia Sinica Institute of Astronomy and Astrophysics and is funded by the Smithsonian Institution and the Academia Sinica.

EVOLUTION AND KINEMATICS OF PROTOSTELLAR ENVELOPES IN THE PERSEUS MOLECULAR CLOUD

Daniel J. Heimsoth (UW Madison), Ian W. Stephens (Worcester State U., CfA), Héctor G. Arce (Yale), Tyler L. Bourke (SKA, CfA), Philip C. Myers (CfA), Michael M. Dunham (SUNY Fredonia)

The process of mass accretion during the earliest stages of protostar development sets the final characteristics of the resultant star and thus is a crucial mechanism to study. Reductively, gas and dust from the parent molecular cloud fall onto the protostellar core, which in turn feeds an envelope on the scale of $\sim 10^2$ - 10^4 au surrounding the protostar. Matter then falls onto the accretion disk (~ 100 au wide), where it can be accreted onto the protostar. Of course, this portrait greatly simplifies the accretion process since other physical phenomena, such as bipolar outflows and angular momentum conservation, significantly affect the kinematics. The mass accretion process also must necessarily evolve in time, as the protostar will eventually stop gaining mass and become a full-fledged star. The protostellar envelope of gas and dust bridges the gap between disk-scale processes (such as outflow production

and mass accretion on the protostar) and the greater molecular cloud environment. There is naturally then much interest in better understanding the evolution, kinematics, and morphology of protostellar envelopes to probe the physics behind mass accretion.

Protostellar evolution is categorized into three stages (c.f. Andre et al. 1993): the Class 0, I, and II stages. The classifications are often separated based on their *bolometric temperature*, T_{bol} , which has been shown to be a relatively good proxy for age (e.g., Myers & Ladd 1993). The separation for Class 0 and I is at $T_{\text{bol}} \approx 70$ K, and the separation for Class I and II is at $T_{\text{bol}} \approx 650$ K. Arce & Sargent (2006) conducted one of the first high-resolution spectral line surveys to investigate how envelopes and their bipolar outflows evolve through time. **Figure 1** shows a cartoon

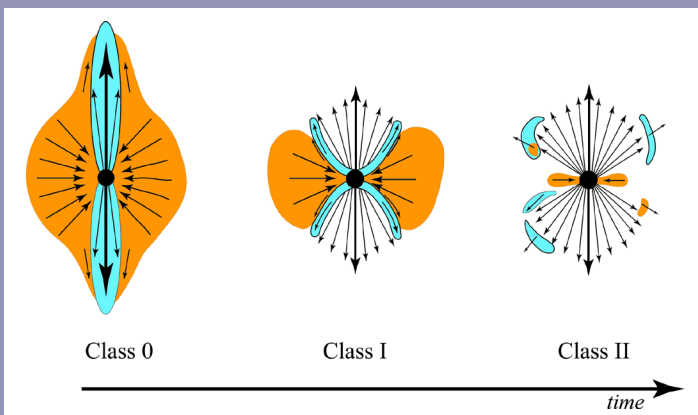


Figure 1: Cartoon adapted from Arce & Sargent (2006). During the Class 0 stage, some of the protostellar envelope (orange) is swept up with the outflow (cyan). At the Class I stage, the outflow has cleared out a cavity and the envelope only appears perpendicular to the outflow. By the Class II stage (not studied in this work), the envelope and outflow have mostly dissipated.

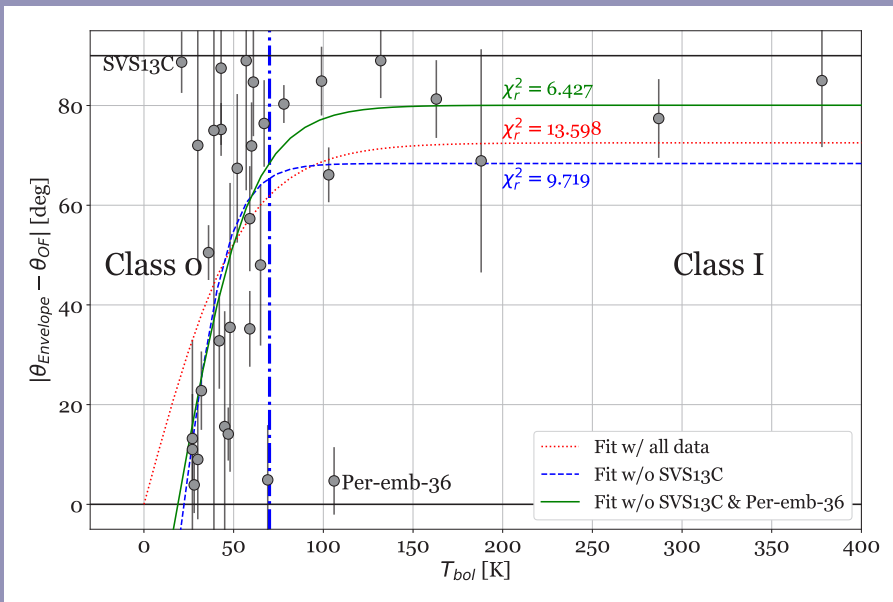


Figure 2: The difference in the elongation angle of the envelope and the position angle of the bipolar outflows versus T_{bol} . The data were fit with a tanh fit using all sources (red dotted), without Per-emb-36 (blue dashed), and without both Per-emb-36 and SVS13C (green solid). We find that with increased T_{bol} the envelopes become more perpendicular to the outflows (and hence more parallel with the accretion disks). The vertical blue line denotes the approximate separation between Class 0 and Class I protostars.

of how the outflows are theorized to affect and eventually destroy the envelope. While their study only looked at nine relatively bright sources, the more recent Mass Assembly of Stellar Systems and their Evolution with the SMA (MASSES) survey imaged the known 74 Class 0 & I protostars in the nearby Perseus molecular cloud in multiple spectral lines and 1.3 mm and 850 μm continuum bands (Stephens et al. 2018, 2019). Class II protostars were not observed because they lack an intact envelope.

In a recently published work (Heimsoth et al. 2022), we used the $\text{C}^{18}\text{O}(2-1)$ spectral line from the MASSES dataset as a tracer for the protostellar envelope to characterize the shapes, sizes, and orientations of 54 envelopes and to measure their fluxes, velocity gradients, and specific angular momenta. The bipolar outflows were mapped in the $\text{CO}(2-1)$ spectral line observed by MASSES using the SMA, and T_{bol} data for the studied protostars were taken from Tobin et al. (2016).

One prediction of the model constructed by Arce & Sargent (2006) (see Figure 1) is that as protostars evolve and transition from Class 0 to I, the protostellar envelope should become flattened by the expanding outflows along the plane of the accretion disk, i.e., perpendicular to the axis of the bipolar outflows. By fitting a 2D Gaussian to the total flux integrated across velocity channels in C^{18}O , we could measure the apparent orientation of the envelope relative to the accretion disk and bipolar outflows. Figure 2 shows the relationship between the angular difference between the principal axis of the envelope (θ_{Envelope}) and the bipolar outflow axis (θ_{OF}) and T_{bol} . Two sources, Per-emb-36 and SVS13C, were found to be outliers and were affecting the goodness of fit of the tanh fit; thus, we show multiple such fits with and without these sources. The best fit results in a transition between non-ori-

ented envelopes (Class 0) and envelopes parallel to the disk (Class I) of $T_{\text{bol}} = 53 \pm 20$ K.

The kinematics of the protostellar envelope can offer insight into the physical processes that move matter between the greater molecular cloud and the accretion disk. Intuitively, we expect the velocity gradient of the system to increase with a decrease in the radius as material falls in towards the center and picks up kinetic energy. To test if this is true for our sample, we used multi-scale data from multiple surveys (Goodman et al. 1993; Chen et al. 2019a; Chen et al. 2019b; Caselli et al. 2002; Chen et al. 2007; Pirogov et al. 2003; Tobin et al. 2011) to study the relation between the radius of the envelope/core and the velocity gradient (Figure 3) and the specific angular momentum (Figure 4). These graphs separate the Perseus sources based on how many protostars are contained in the envelope and how close they are. Definitions of the three designations (single, close binary, medium binary) can be found in the paper (Heimsoth et al. 2022).

In Figure 3, we found a significantly higher slope, $|G| \propto R_{\text{eff}}^{-0.72 \pm 0.06}$, compared to previous studies. Should conservation of angular momentum hold and assuming solid-body rotation, we would expect the gradient to go as R^{-1} . The fact that we find a lower scaling suggests a dissipation of angular momentum as material falls in towards the disk, which could be caused by bipolar outflows and/or tension in the magnetic field lines. Furthermore, gas is constantly falling onto the disk and being pulled onto the envelope from the core, which makes it difficult to define the envelope as its own entity that is separate from the rest of the system.

In contrast to the velocity gradient, we expect the specific angular momentum to increase with increasing radius,

$J/M \propto |G|R^2$. We find in Figure 4 that $J/M \propto R^{1.83 \pm 0.05}$, which lies between the expected relations for solid-body rotation ($J/M \propto R^2$) and for turbulence ($J/M \propto R^{1.5}$). This is to be expected, as the envelope gas gains angular momentum from the infalling gas from the core, while dissipative processes provide turbulence in the system. Past studies, such as Belloche (2013), have posited that at scales smaller than ~ 5000 au, the specific angular momentum will be constant. This turnover in the power law is necessary to couple the turbulent dynamics of the core and envelope with the flattened inner disk. Our data cannot rule out such a flattening occurring in the region of ~ 1000 au, as the composite fit in Figure 4 is statistically comparable to the simple power law relation.

While our work offers insights into the physical processes that affect mass accretion on young protostars, there is much opportunity for further study. For example, more observations of gaseous structures near the transition between envelope and disk scales could offer evidence for the theorized turnover of the specific angular momentum power law. In addition, other molecular clouds besides Perseus can be studied in a similar fashion as we have done to increase the statistics. Future work can use the excellent spectral and angular resolution of the SMA to test the results of our work and increase our knowledge of mass accretion processes in protostellar systems.

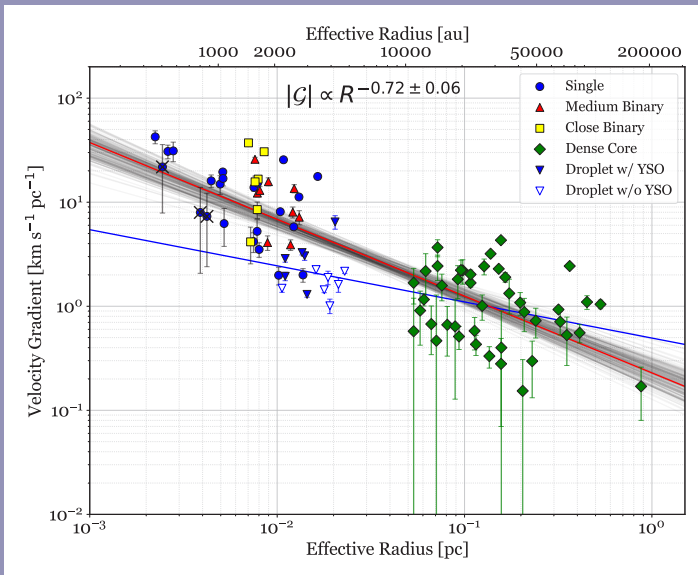


Figure 3: Velocity gradient versus effective radius for Perseus $C^{18}O$ envelopes (solid blue circles, red triangles, yellow squares) from this work, ‘droplets’ (blue solid and hollow triangles) from Chen et al. (2019a), and dense cores (green diamonds) from Goodman et al. 1993. The red line is the best fit for all points, found using a MCMC sampling method. The blue line is the best fit from Chen et al. (2019b) for only the droplets and dense cores.

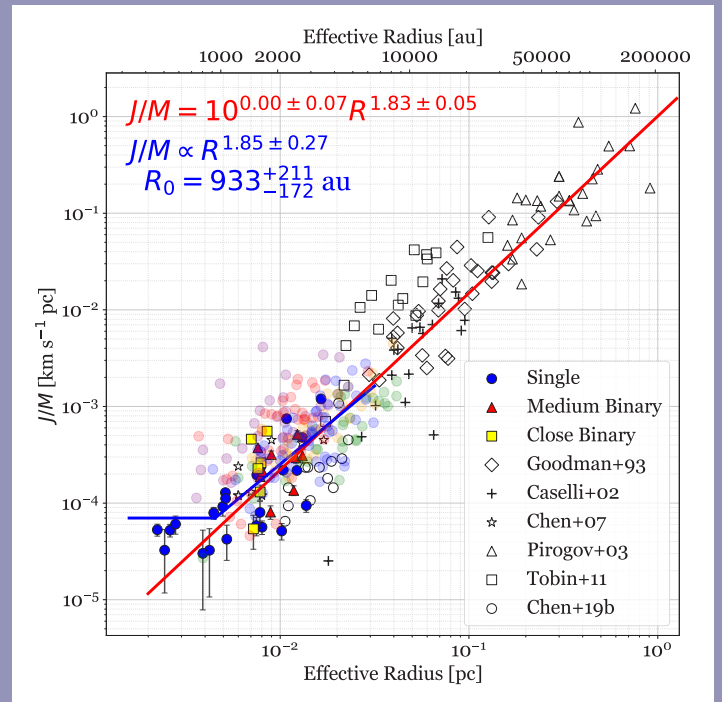


Figure 4: Specific angular momentum as a function of effective radius of the $C^{18}O$ envelopes from this work (solid colors, color-coded by multiplicity), along with data from previous studies (Goodman et al. 1993; Caselli et al. 2002; Chen et al. 2007; Pirogov et al. 2003; Tobin et al. 2011; Chen et al. 2019b) and simulation data from Chen & Ostriker (2018) (translucent circles). We fit both a simple power law fit to all observed data (i.e. not simulated points), shown in red, and a composite power law with cutoff to envelope-scale data (this work; Chen et al. 2007; Chen et al. 2019b), shown in blue. The data are not inconsistent with a flattening of the relation at small scales.

REFERENCES

- Andre, P., Ward-Thompson, D., & Barsony, M. 1993, ApJ, 406
- Arce, H. G., & Sargent, A. I., 2006, ApJ, 646, 1070
- Belloche, A. 2013, EAS Publication Series, 62, 25
- Caselli, P., Benson, P. J., Myers, P. C., & Tafalla, M. 2002, ApJ, 572, 238
- Chen, C.-Y., & Ostriker, E. C. 2018, ApJ, 865, 34
- Chen, H. H.-H., Pineda, J. E., Goodman, A. A., et al. 2019a, ApJ, 877, 93
- Chen, H. H.-H., Pineda, J. E., Offner, S. S. R., et al. 2019b, ApJ, 886, 119
- Chen, X., Launhardt, R., & Henning, T. 2007, ApJ, 669, 1058
- Heimsoth, D. J., Stephens, I. W., Arce, H. G., et al. 2022, ApJ, 927, 88
- Myers, P. C., & Ladd, E. F. 1993, ApJL, 413, L47
- Pirogov, L., Zinchenko, I., Caselli, P., Johansson, L. E. B., & Myers, P. C. 2003, A&A, 405, 639
- Stephens, I. W., Dunham, M. M., Myers, P. C., et al. 2018, The Astrophysical Journal Supplemental Series, 237, 22
- Tobin, J. J., Hartmann, L., Chiang, H.-F., et al. 2011, ApJ, 740, 45
- Tobin, J. J., Looney, L. W., Li Z.-Y., et al. 2016, ApJ, 818, 73

CORE MASS FUNCTION OF A SINGLE GIANT MOLECULAR CLOUD COMPLEX WITH $\sim 10,000$ CORES

Yue Cao, Keping Qiu, Qizhou Zhang, Yuwei Wang, and Yuanming Xiao

The universality of the stellar initial mass function (IMF) has intrigued astrophysicists for many decades in pursuing its origin (Salpeter 1955; Kroupa et al. 2013; Offner et al. 2014). Stars assemble their masses from molecular clouds. Observational studies on Galactic star-forming regions found that the mass distribution of cores—dense, elliptical structures on 0.01–0.1 pc scales—has a shape similar to the IMF but is shifted systematically toward higher masses by a factor of ~ 3 (Motte et al. 1998; Testi & Sargent 1998; Alves et al. 2007; Könyves et al. 2015). This discovery prompts the intuitive idea that IMF originates from the core mass function (CMF) via a self-similar core-to-star mass mapping process, i.e., the probability that a core forms a star is constant as long as the core-to-star mass ratio is constant (Motte et al. 1998; Alves et al. 2007; Motte et al. 2018). To understand this resemblance and how it is related to the origin of the IMF, it is essential to accurately determine the shape of CMF with a large sample size and resolve the core fragments with high-resolution observations.

The Cygnus X giant molecular cloud (Cyg X) is one of the nearest (~ 1.4 kpc; Rygl et al. 2012), largest (~ 130 pc), and most massive molecular cloud complexes in the Milky Way. It has a total molecular mass of $\sim 3 \times 10^6 M_{\odot}$ (from Cao et al. 2019), and is representative of the active high-mass star-forming regions in the spiral arms, and is thus an ideal target for constructing a large sample of cloud structures. The identification of cores in Cyg X was conducted on an H_2 column density ($N_{(H_2)}$) map illustrated in **Figure 1**, which was generated by Cao et al. (2019) with the hirescoldens procedure (Men'shchikov et al. 2012) that fits pixel-by-pixel the Herschel continuum images with a graybody thermal dust emission model (Hildebrand 1983). The map provides abundant and detailed

information of the spatial distribution of the cold molecular gas in Cyg X with a dynamic range of 1300 in spatial scale (0.14–180 pc) and 1000 in column density (4×10^{20} – 4×10^{23} cm^{-2}).

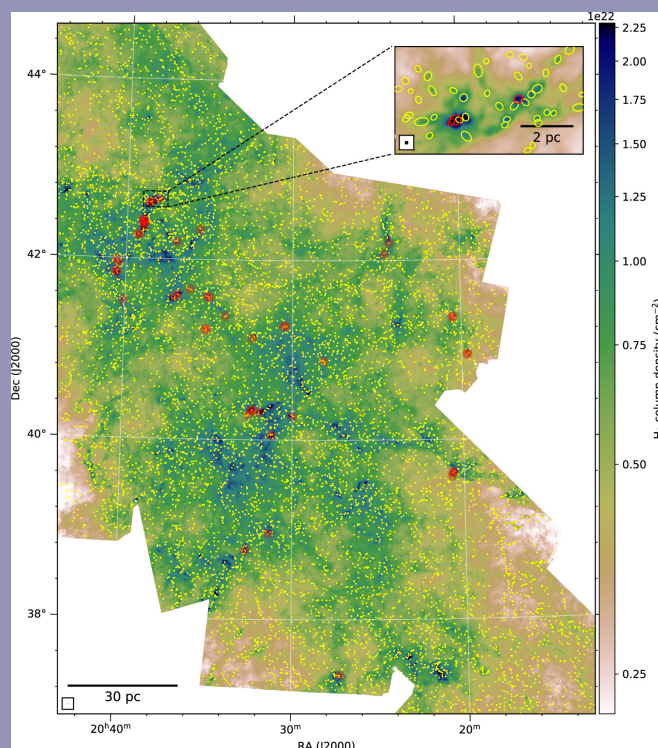


Figure 1: H_2 column density map of the Cyg X region and the 8,000+ cores extracted as dots (main panel) or ellipses (zoomed-in panel), of which the targets of SMA are marked in red.

We used the getsources algorithm (Men'shchikov et al. 2012) to extract cores in Cyg X and found 8,431 robust cores. Their mass function is shown in Figure 2.

How do cores distribute their masses into stars in light of the resemblance among their mass functions? Since it is impossible to trace the whole lifetime of a core observationally, here we focus on the observable core-to-condensation fragmentation to address this problem. Mathematically, there are infinite numbers of ways of core-to-condensation mass mapping even if the two mass functions are identical in shape. Among all the possibilities two intuitive mapping scenarios have been proposed in the literature: (1) self-similar mapping (Motte et al. 1998; Alves et al. 2007; Motte et al. 2018), where the probability that a core of mass M_c forms a condensation of mass M_{cd} is constant as long as M_{cd}/M_c is constant; and (2) internal-IMF mapping (Beuther & Schilke 2004; Shadmehri & Elmegreen 2011), where the underlying condensation mass function (CdMF) in each core is identical to the IMF. To check the validity of these scenarios, we conducted a high-resolution pilot survey toward 48 selected cores with the SMA in 1.3 mm, aiming at resolving the cores into condensations with a synthesized beam of $\sim 1''8$ ($0.012 \text{ pc}@1.4 \text{ kpc}$), which is more than one order of magnitude smaller than the average core diameter. The target cores were chosen in the high-mass range of the core sample ($>10 M_\odot$) for better detections and to better demonstrate the mass mapping in the more featured and reliable power-law part of the CMF. They were also selected to be absent from the strong free-free emissions of the ultracompact HII regions in Cyg X (Cao et al. 2019) so that the condensation masses can be properly estimated with the continuum fluxes, which are dominated by thermal dust emissions. Figure 1 presents the spatial distribution of the target cores in Cyg X and their 1.3 mm continuum images are shown in Figure 3. We use getsources to identify condensations in the SMA images and selected 200 robust condensations with 5σ detections. To generate the core-condensation correspondence, we associated each condensation with the nearest core of which the FWHM ellipse covers the condensation. As a result, 180 condensations are associated with the 48 target cores.

Figure 4 presents the core mass versus condensation mass relation. Regression analysis on the mean condensation mass in each core versus the core mass yields $M_{cd,av} \propto M_c^{0.27 \pm 0.14}$ with a low correlation coefficient of $R = 0.27$, which is different from the $M_{cd,av} \propto M_c$ relation predicted by the self-similar mapping model. To further corroborate this difference, we ran Monte Carlo simulations to generate pseudo condensation masses for each core following the self-similar mapping routine, with the condensation numbers and core-to-condensation formation efficiency mimicking the real data. After 500 iterations we derive a mass relation with the pseudo data:

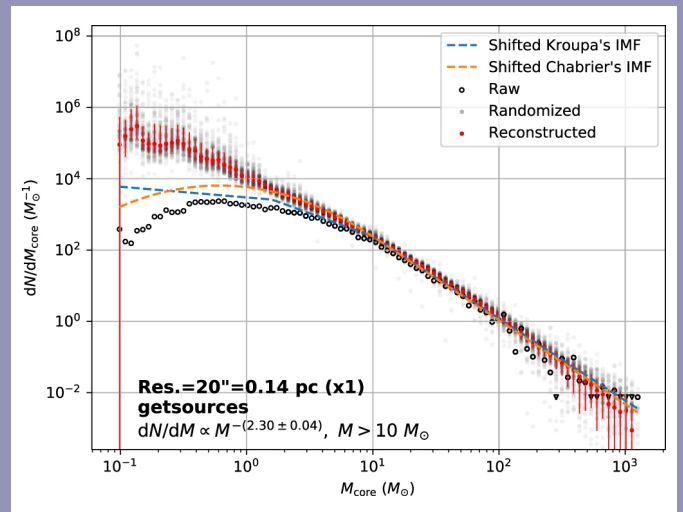


Figure 2: Raw (black circles) and completeness-corrected (red dots) CMFs of Cyg X. Shifted IMFs are also shown. The error bars of the corrected CMF (red dashes) were derived considering the mass uncertainty, the binning uncertainty, and the statistical errors.

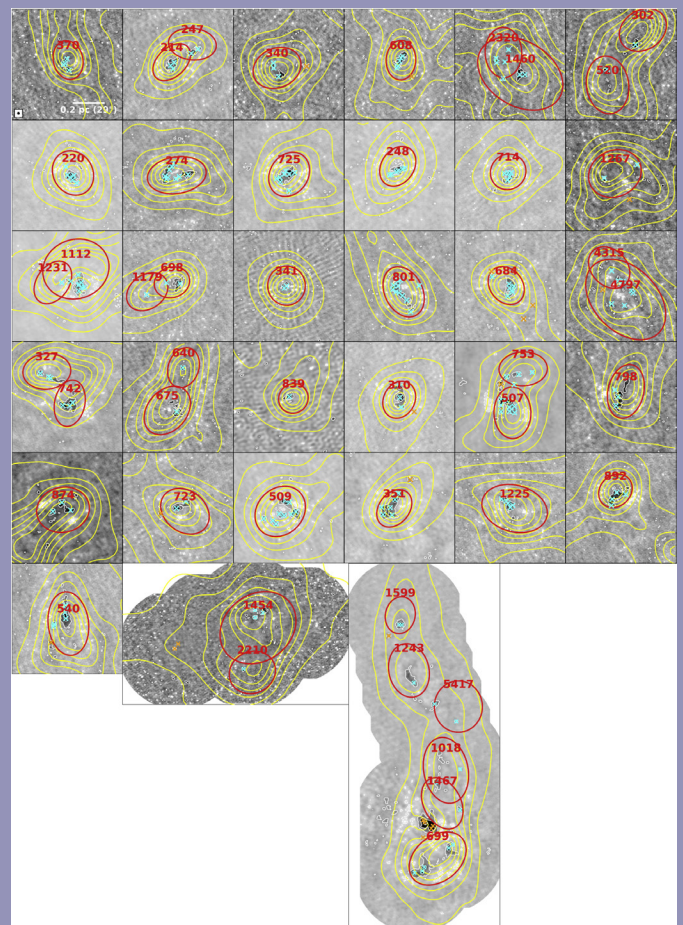


Figure 3: SMA 1.3 mm continuum observations of the target cores in Cyg X. Yellow contours are of the H_2 column densities derived from the Herschel data. Red ellipses show the FWHM sizes of the cores. Cyan and orange crosses represent the fragments associated/not associated with the cores, respectively.

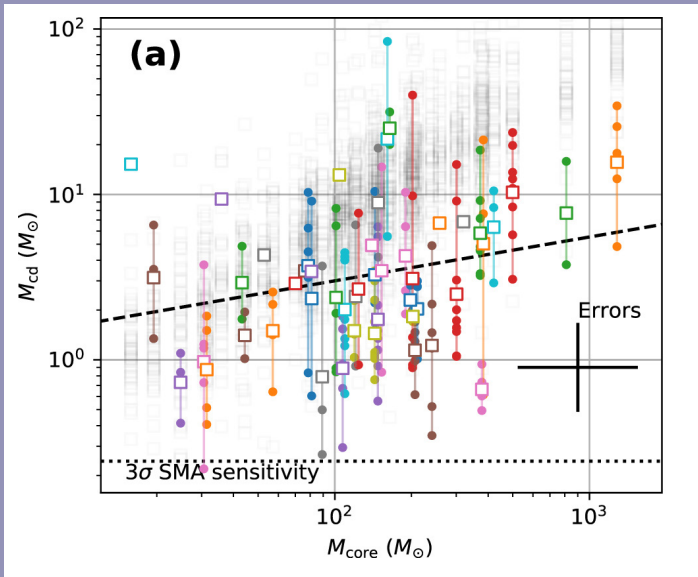


Figure 4: Core mass vs the masses of the fragments showing that the self-similar mapping is not the case here. Each group of monochromatic dots is for each core. Squares are the averaged values. The dashed line is a linear fitting of the data. Gray translucent squares show the pseudo data generated by Monte Carlo simulations of the self-similar core-to-condensation mass mapping model.

$M_{cd,av} \propto M_c^{1.0 \pm 0.11}$, which indicates that the observed core-to-condensation mass mapping is highly unlikely to be reproduced by the self-similar model. To examine the validity of the internal-IMF model, we performed the two-sided Kolmogorov–Smirnov test with the core/condensation masses as input and with the null hypothesis that the CdMF in each core has the shape of the IMF regardless of the core mass. The derived p-value is 0.014, which indicates that this model cannot reproduce the observed results. Moreover, the mass distribution of condensations in each core greatly varies from

case to case, and is clearly different from the IMF, apparently inconsistent with the internal-IMF model. The cumulative CdMF of all the condensations from all the observed cores has a shape relatively more comparable with the IMF, but there is still deviation in between. The evidence against both scenarios proposed in the literature points to the chaotic nature of the core-to-condensation (and probably also core-to-star) mass mapping process, and implies that any scenario proposed without full understanding of the underlying physics may oversimplify the reality and fail to explain it.

REFERENCES

- Alves, J., Lombardi, M., & Lada, C. J. 2007, *A&A*, 462, L17
- Beuther, H., & Schilke, P. 2004, *Sci*, 303, 1167
- Cao, Y., Qiu, K., Zhang, Q., et al. 2019, *ApJS*, 241, 1
- Hildebrand, R. H. 1983, *QJRAS*, 24, 267
- Könyves, V., André, P., Men'shchikov, A., et al. 2015, *A&A*, 584, A91
- Kroupa, P., Weidner, C., Pflamm-Altenburg, J., et al. 2013, in *The Stellar and Sub-Stellar Initial Mass Function of Simple and Composite Populations*, ed. T. D. Oswalt & G. Gilmore, Vol. 5 (Berlin: Springer), 115
- Men'shchikov, A., André, P., Didelon, P., et al. 2012, *A&A*, 542, A81
- Motte, F., Andre, P., & Neri, R. 1998, *A&A*, 336, 150
- Motte, F., Nony, T., Louvet, F., et al. 2018, *NatAs*, 2, 478
- Offner, S. S. R., Clark, P. C., Hennebelle, P., et al. 2014, in *Protostars and Planets VI*, ed. H. Beuther et al. (Tucson, AZ: Univ. Arizona Press), 53
- Salpeter, E. E. 1955, *ApJ*, 121, 161
- Shadmehri, M., & Elmegreen, B. G. 2011, *MNRAS*, 410, 788
- Rygl, K. L. J., Brunthaler, A., Sanna, A., et al. 2012, *A&A*, 539, A79
- Testi, L., & Sargent, A. I. 1998, *ApJL*, 508, L91

A LOOK AT THE wSMA RECEIVER CARTRIDGE

wSMA Team: Paul Grimes, Edward Tong and Lingzhen Zeng

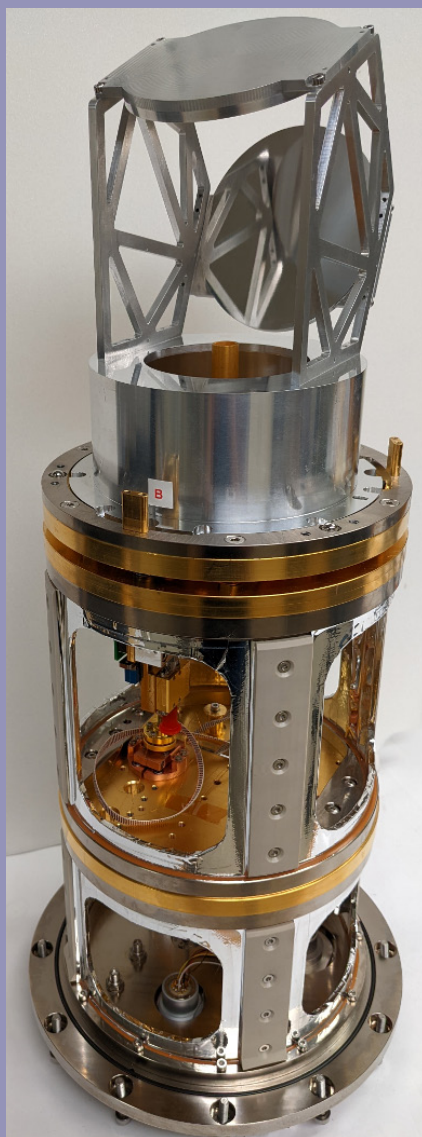


Figure 1: Photo of a wSMA Receiver Cartridge.

In the previous newsletter, we have reported on the Status of new Cryostat for the wSMA (Tong et al. 2021). Each cryostat carries two dual-polarization receiver cartridges. Here we present in more detail the features of the receiver cartridge. A photo of the receiver cartridge is shown in Fig. 1.

A selector wheel inside the wSMA cryostat directs the signal beam from the SMA antenna's beam waveguide towards each of the two receiver cartridges (Grimes et al. 2020). The incident beam is refocused by a receiver optics module, which occupies the top part of each cartridge.

Referring to Fig. 2, the receiver optics module consists of two offset hyperboloid mirrors, arranged as a clamshell mirror pair, which reimages the virtual image of the telescope aperture generated by the SMA antenna's beam waveguide onto the receiver feed horn aperture. By the use of the Fresnel imaging equations and the Mizuguchi-Dragone condition, the mirror pair is designed to produce a frequency independent image of the telescope aperture, with minimal cross-polarization. (As with the original SMA optics, the telescope is fed from a pupil plane rather than an image of the sky in order to maximize single-pixel aperture efficiency at all frequencies.) The aluminum mirror pair is mounted by an aluminum space frame structure and "drum" that surrounds the feed horn and the frontend assembly which will be described below.

The receiver feed horn is designed so that its aperture field amplitude and phase optimally matches the pupil image presented by the optics. This requires a flatter than usual phase profile at the feed aperture, which is accomplished through the use of a profiled corrugated feed horn design.

At the heart of the cartridge is a front end assembly, located just below the feed horn. The front end assembly houses the waveguide orthomode transducer (OMT) and the waveguide

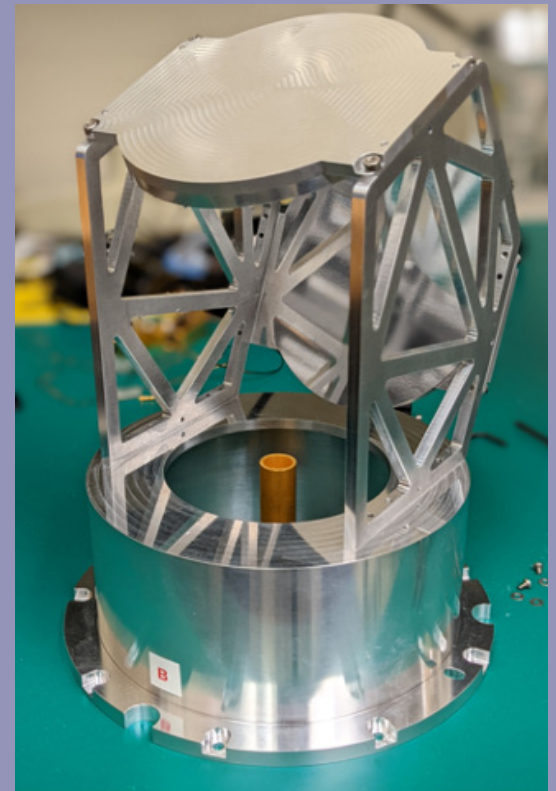
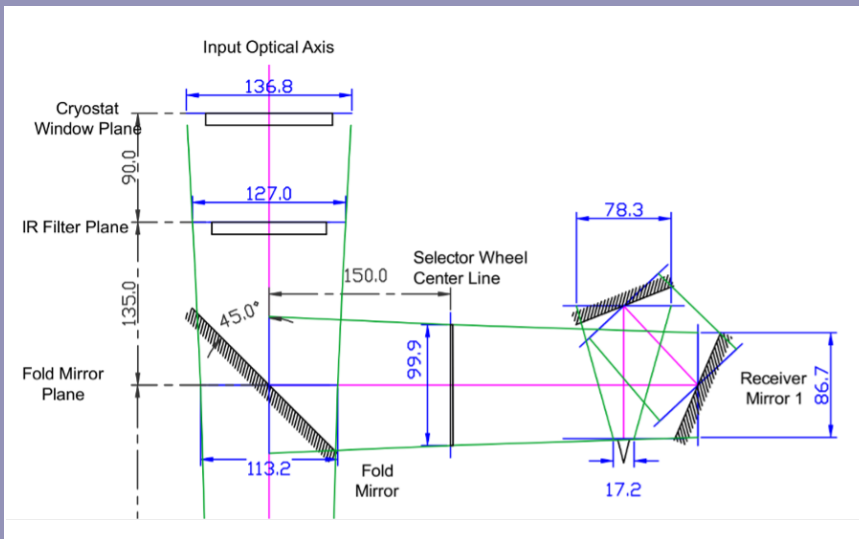


Figure 2: (Left) wSMA Cryostat and Receiver Optics layout. The center of the optical beam is shown in pink, while the maximum extent of the beam is shown in green. Dimensions are in mm. (Right) wSMA Receiver Optics assembly with wSMA profile Feedhorn mounted at its center.

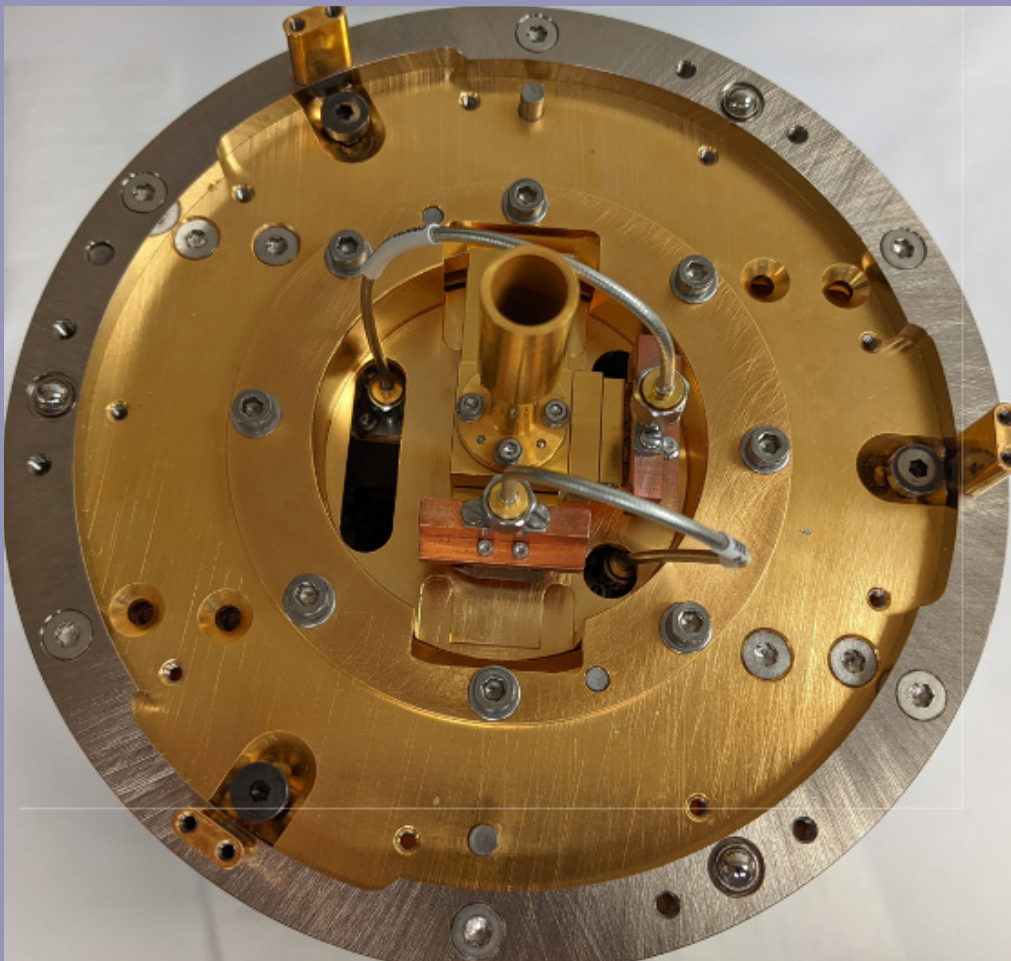


Figure 3: Top view of the floating 4 K plate of the receiver cartridge with the receiver optics removed. The frontend assembly is bolted on an interface plate in the center. The profiled feedhorn is mounted on its top. The two mixer blocks carrying the SIS mixer, one for each polarization, are mounted on its side. Slots in the interface plate allow flexible cables to carry the IF signal to the isolator and LNA assembly mounted to the fixed 4 K plate below. LO power is injected into the front end assembly through two waveguide ports on the bottom of the frontend assembly.

circuit for local oscillator (LO) injection. The OMT splits the incoming wave into two linearly polarized outputs, each of which is directed to an LO coupler based on a novel design employing a silicon coupler chip (Zeng et al. 2020). The LO power enters from the base of the front end assembly through a pair of waveguide ports. Referring to Fig. 3, a pair of mixer blocks carrying the SIS mixer chips, one for each polarization, are attached to the sides of the assembly. The downconverted intermediate frequency (IF) outputs from the mixer blocks are connected to the IF section through a pair of flexible coaxial cables.

Both the receiver optics module and its space frame as well as the frontend assembly are all mounted on a mechanically floating 4 K stage of the cartridge, which is connected to the fixed 4 K plate of the cartridge through a pair of flexible heat straps and springs. This arrangement allows the receiver optics to be registered under spring pressure to the top plate of the cryostat, which in turn is referenced to the rest of the SMA antenna's beam waveguide setup, ensuring consistent optical alignment. The fixed 4 K plate of the cartridge is connected to the 4 K cold plate of the wSMA cryostat via an automatic thermal link. A pair of cryogenic isolators (Zeng et al. 2018) and low noise amplifiers (LNAs) are mounted below

the fixed 4 K plate and are connected to the mixer blocks via flexible coaxial cables. The temperature difference between the fixed and floating 4 K stages is typically 0.1 K.

The 50 K stage lies below the 4 K fixed plate. This is connected to the 50 K plate of the cryostat via a second automatic thermal link. A pair of stainless steel overmoded waveguides carrying LO power for the SIS mixer; coaxial cables carrying the LNA outputs, and cryogenic ribbon cables carrying SIS and LNA biasing and thermometry are all heat sunk into this stage before continuing on to room temperature. Our thermal model shows that the conducted heat load between the 50 and 4 K stage of each cartridge is around 130 mW.

Finally, on the bottom of the cryostat, we have the various connectors, including two waveguide ports, four coaxial connectors (including two for future expansion) as well as three connectors for thermometry, mixer and LNA bias. The wSMA cryostat is equipped with a cartridge loader which allows the cartridge to be pushed into the cryostat easily from the bottom. Once the cartridge is in place, guide rails are mounted to its base and an LO module, which also carries the first stage room temperature IF amplifiers, can easily be installed.

REFERENCES

- E. Tong, P. Grimes, and L. Zeng, "Status of new Cryostat for wSMA," SMA Newsletter, p 15, July 2021.
- P. K. Grimes, S. N. Paine, L. Zeng, and E. C.-Y. Tong. "Optics and Feed Design for the wSMA Receiver System," Proceedings of the 31st International Symposium on Space THz Technology (ISSTT2020), Tempe, AZ, 2020.
- L. Zeng, W. C. Lu, P. K. Grimes, T. J. Chen, Y. P. Chang, C.-Y.E. Tong, and M. J. Wang, "A silicon chip-based waveguide directional coupler for terahertz applications," IEEE Transactions on Terahertz Science and Technology, 10(6):698–703, 2020.
- L. Zeng, C.E. Tong, R. Blundell, P.K. Grimes, and S.N. Paine, "A Low-Loss Edge-Mode Isolator With Improved Bandwidth for Cryogenic Operation," IEEE Transactions on Microwave Theory Techniques, 66(5):2154–2160, May 2018.

RTDC NEWS

Holly Thomas

A New SMA Archive

The Radio Telescope Data Center (RTDC) is pleased to introduce the new SMA science archive. From early August, 2022, visitors to the online archives - public and proprietary - will find them completely redesigned, with new interfaces, faster response times, and expanded search options. Upon requesting datasets, SMA users will discover options to receive the data in CASA Measurement Set, alongside the native raw MIR/IDL format. In addition, available request options will include binning spectral channels and the application of system temperatures and flagging tables.

These new options are only the first stage of a planned expansion of functionality for the archives, with further upgrades being incrementally released over the next few months. In this first step, these new options will only be available for data taken after July 2019 (corresponding to the most recent version of the data acquisition software). It will therefore include all data in the proprietary archive which goes back 15 months, along with the public data in the most recent years (summer 2019 – spring 2021). Future updates will expand the data range back to 2017, and eventually back further to the start of the SWARM correlator in 2014. Data not available through these new paths will continue to be downloaded in the native MIR/IDL format. Other changes to look out for in upcoming releases will be the capability to request data at higher calibration levels.

This new archive is a complete redesign and will provide the infrastructure to support further development with more flexibility in the future. In addition to increasing the range of data products we can make available, it also allows for more responsive data patching, easier communication with our users, and more advanced data retrieval features such as source and spectral line extraction.

The goal of this project has been to lower barriers to the publication of SMA data for both current and future SMA users.

The native format of SMA data is MIR/IDL, with MIR being an IDL based software package tailored to work uniquely with SMA data. This has served us well for many years. However, the software landscape of astronomy is changing and the limitations of MIR now represent significant obstacles. Most notably, MIR requires an IDL license which many institutions no longer support; additionally, MIR is designed to read the full dataset into memory before executing any operations. With the growing data sizes at the SMA, now often exceeding 150GB for a single observation, this severely stretches hardware resources.

With more users turning to CASA as the primary tools for interferometric data reduction, there has been a growing demand among our user base to use CASA for processing SMA data. We have offered pathways to do this for several years, but they have still required MIR/IDL as an intermediate step. With CASA recognized as the software of choice for interferometry, the SMA has been working hard to make this conversion easier and more robust. We are now delighted to be able to offer data in Measurement Set format directly from the online archives.

Introducing pyuvdata

This ability to offer SMA data in CASA Measurement Set format is due to pyuvdata, a software package that offers a pythonic interface to interferometric data sets. The goal of this software is to allow high quality conversion between interferometric data formats. This is an ongoing project that will continue to grow in capability and scope. Initially developed by these in the low frequency 21cm community (Hazelton et al., 2017), the full range of options currently includes reading and writing of miriad, uvfits, CASA Measurement Sets and uvh5 data, and reading of FHD (Fast Holographic Deconvolution) visibility save files, SMA MIR/IDL data, and MWA correlator FITS files. See <https://pyuvdata.readthedocs.io/en/latest/index.html> for full details.

Figure 1: New public archive search form.

# Bsls	Ang. res.	Pol	Project code	PI	Raw size	Observing report
15	2.9"	0	2021A-S028	Ashby	62.0G	Proprietary
15	2.9"	0	2021A-S028	Ashby	62.0G	Proprietary
15	2.9"	0	2021A-S028	Ashby	62.0G	Proprietary
15	2.9"	0	2021A-S028	Ashby	62.0G	Proprietary
15	2.9"	0	2021A-S028	Ashby	62.0G	Proprietary
15	2.9"	0	2021A-S028	Ashby	62.0G	Proprietary
15	2.9"	0	2021A-S028	Ashby	62.0G	Proprietary
15	2.9"	0	2021A-S028	Ashby	62.0G	Proprietary
15	2.9"	0	2021A-S028	Ashby	116.8G	Proprietary
15	2.9"	0	2021A-S028	Ashby	116.8G	Proprietary
15	2.9"	0	2021A-S028	Ashby	116.8G	Proprietary
15	2.9"	0	2021A-S028	Ashby	116.8G	Proprietary
15	2.9"	0	2021A-S028	Ashby	116.8G	Proprietary
15	2.9"	0	2021A-S028	Ashby	116.8G	Proprietary
15	2.9"	0	2021A-S028	Ashby	116.8G	Proprietary
28	3.3"	0	2018B-S029	Watanabe	40.4G	obs report
28	3.8"	0	2018B-S029	Watanabe	2.5G	obs report

Figure 2: New public archive results page.

The inclusion of the SMA MIR data format into the fold has been the result of months of work by the SMA and pyuvdata teams. It is a project that remains under development but for this first release of the new SMA archives, we are happy to be able to offer SMA data in Measurement Set format through the online web-forms, along with optional rechunking, and application of the system temperature corrections and flagging table. The option to request rechunked data is especially important for SMA users - our high spectral resolution of 140kHz can result in large file sizes which may not be necessary for some science goals. Typically, around 75% of proprietary data requests want some level of rechunking applied. Functionality will continue to be added over the coming

months. In particular, we look forward to offering calibrated datasets with bandpass and gain calibrator solutions applied.

The gain solutions themselves are generated by our in-house software package COMPASS. COMPASS was designed as a quality assessment tool to be used by staff in order to identify potential issues with the array, and PIs will have noticed these reports available on their observation pages in the SMA Observer Center. As part of this assessment process, COMPASS generates the gains solutions, then makes dirty images for each source. Clearly, if pyuvdata can be adapted to apply gain solutions during the conversion to Measurement Sets we can use these packages in combination to provide users with calibrated data. To this end, we are currently

working through the practicalities of building a database of gains solutions and applying them on demand, as well as upgrading pyuvdata to generate CASA calibration tables. With so much effort focused on these tasks we hope to offer calibrated measurement sets by the end of the year.

Note that pyuvdata is open-source and available to any of our users through conda. It is very well documented and users can visit the pyuvdata web page (<https://pyuvdata.readthedocs.io/en/latest/uvdata.html>) for a complete overview and examples, the Github page (<https://github.com/RadioAstronomySoftwareGroup/pyuvdata/>) for installation instructions, and the RTDC pyuvdata page (<https://lweb.cfa.harvard.edu/rtdc/SMAdata/process/pyuvdata/>) for SMA specific information and examples.

Archive Redesign

The public and proprietary SMA web archives have been completely redesigned to coincide with the pyuvdata release thereby offering not only a faster response time with expanded search options, but also a broader range of data products.

The archives have a new backend built on a MySQL database, with python based front-ends to accept data requests through web-forms. These scripts interact with the database, display the result, execute user requests, then pass the data back to the user via an email. This does require users who request data in this way to enter an email address at which they will receive a download link.

The SQL database has been a huge part of reducing the wait time on searches, which under the previous incarnation could take up to 30 seconds. With this new setup, searches have been sped up by a factor of 5-20, depending on the number

of results returned. The switch to a SQL format opens the door for future relational database functionality, this will allow further integration between the RTDC and SMA software.

Visitors to the public archive will notice a number of new search options, including a CDS Sesame name resolver, a project title keyword search, and a 'public data only' search flag (see [figure 1](#)).

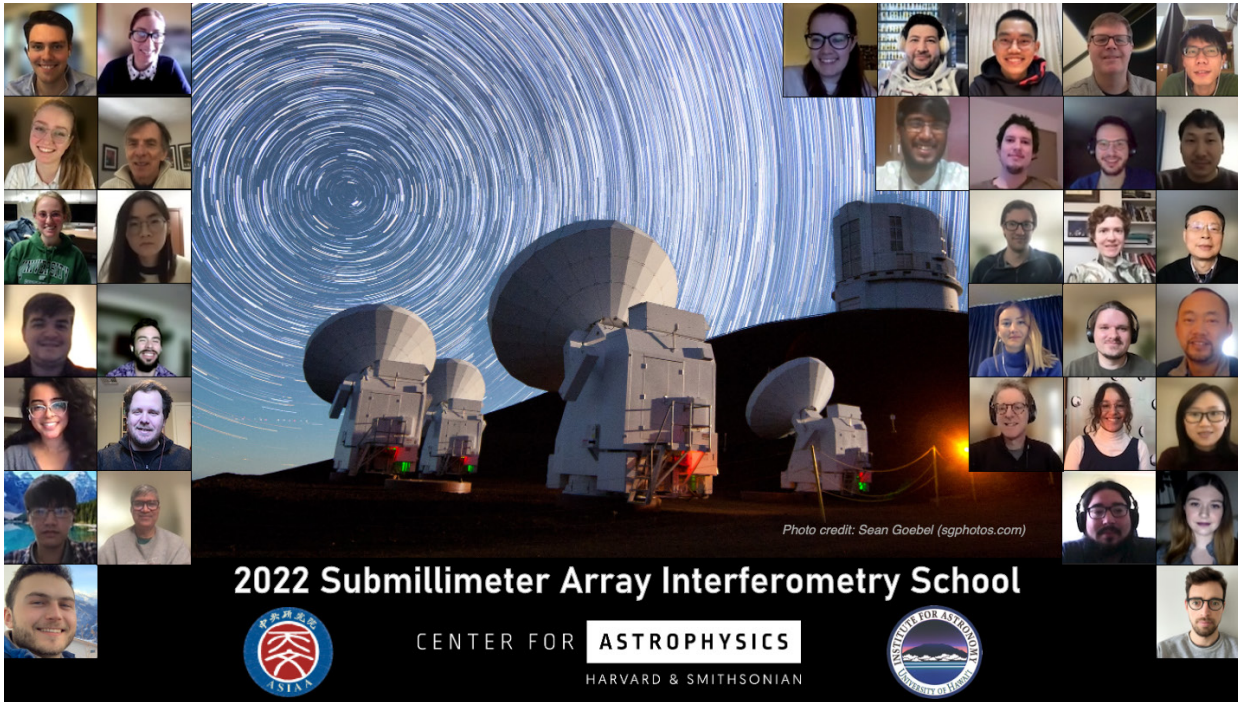
New features are also available to improve interactions with the results (see [figure 2](#)). We now offer users advanced text search, sorting, and display options. For searches based on coordinates, users will see a sky view option which utilizes AladinLite to display the results on a sky image (<https://aladin.u-strasbg.fr/AladinLite/>). Users will also find buttons to show/hide the search form and change the column visibilities, while those who want to examine the results offline can print them in CSV format.

Visitors to the proprietary archive will find the same new look and download options. To access proprietary data, you must be the PI or an authorized user (co-I) on the given project, and provide the project code and your email. This will be the email used to create your account in the SMA Observer Center.

These improvements to SMA data accessibility and usability are an ongoing project that we expect to build on not just over the coming months but the coming years. Some of features we hope to offer will require more fundamental changes to the data acquisition process and the computing infrastructure on Maunakea and are necessarily longer term projects. The SMA is committed to make our data more convenient for our users by expanding both the range and quality of the data on offer. We encourage readers to follow our progress on the RTDC web pages as well as in future newsletters.

REFERENCES

- Hazelton et al., The Journal of Open Source Software, Feb. 2017, vol. 2, issue 10, id. 140.



2022 SUBMILLIMETER ARRAY INTERFEROMETRY SCHOOL

The Center for Astrophysics, in conjunction with the Academia Sinica Institute of Astronomy and Astrophysics and the University of Hawaii, held the Submillimeter Array Interferometry School from January 18 - 22, 2022. The school was conducted virtually, with instructors joining in from across the globe. The SMA Interferometry School aims to provide advanced undergraduates, graduate students, post-docs and early career scientists outside the field with a broad knowledge of interferometry and data reduction techniques at millimeter and submillimeter wavelengths. This year's school hosted a total of 36 students from 25 different institutions and 10 different countries.

This year, students were trained through a mixture of lectures, as well as online discussion sessions and data reduction training sessions. Each student was able to conduct observations with the SMA, the results of which were shown at the conclusion of the week-long workshop. The students produced several impressive results from a wide array of astronomical targets, from nearby star-forming regions to the detection of distant galaxies in the early Universe.

Presentations from the lectures of the school, including slides and recordings, can be found here:

<https://www.cfa.harvard.edu/sma-school/program>

The organizing committee wishes to thank all those who helped to put on the school, as well as all those who attended. Those who are interested in participating in the SMA Interferometry School in the future are encouraged to contact sma-school@cfa.harvard.edu for further information. An announcement for the 2023 SMA Interferometry School is anticipated by the beginning of Fall 2022.

STAFF CHANGES IN HILO

Adrien Diven, Electronics Technician, rejoined SAO in April, reporting to Rob Christensen. He recently worked at the VLBA and the VLA and, before that, worked at the SMA from 2004 to 2015. Welcome back!

Ram Rao, Physicist, moved to the SMA group in Cambridge in June. As an SAO postdoc, ASIAA staff, and then SAO staff, Ram has worked at the SMA in Hilo for 19 years. His many contributions to the telescope include tireless work to implement and improve the polarization capabilities. Most recently, he has overseen nightly observations and ably supervised and trained the operators during a difficult period.

JOHN MAUTE RETIRES AFTER 25 YEARS AT SMA

John Maute, Electrical Engineer, retired at the end of June, more than twenty five years after he joined the SMA. Prior to joining SAO, John worked at two other Maunakea observatories, the CSO and at the Keck Observatory. At the SMA, John initially worked with antenna development at Haystack. He then moved back to Hilo in 1999, where he developed and supported critical systems as the telescope progressed from initial antenna assembly through testing and commissioning into full operations. His many areas of expertise include the observatory electrical systems, the antenna drive systems, the transporter, mechanical systems, chillers, telephones, fire alarms, and ventilation and a/c systems. He kept these complex, heterogeneous systems running despite a seemingly continuous stream of external interruptions and unexpected outages. In recent years, he ably supervised many of the technicians.

Thank you, John, for your contributions to the SMA over all these years. Happy Retirement!

SMA POSTDOCTORAL FELLOWS: COMINGS AND GOINGS

The Submillimeter Array Postdoctoral Fellowship program supports early career scientists active in a variety of astronomical research fields involving submillimeter astronomy. The SMA Fellowship is competitive, and a high percentage of our past Fellows have gone on to permanent faculty and research staff positions located around the world.

The SMA welcomes our newest Fellows:

Joshua Lovell is finishing his Ph.D. work at Cambridge University, with the thesis 'High resolution studies of planetary systems' (advisor: Mark Wyatt). Joshua's research is focused on gas and dust in protoplanetary disks around pre-main sequence stars, and their evolution.

Jakob den Brok is finishing his Ph.D. work at University of Bonn, Germany, with the thesis 'Molecular Gas Physics and Chemistry Across Nearby Galaxies' (adviser: Frank Bigiel). Jakob's research is in observational astronomy related to interstellar medium in galaxies, with particular interests in studying the molecular gas in nearby galaxies.

Lovell and den Brok will take up their fellowship in fall 2022. They join continuing SMA Fellows Eric Koch and Kirsten Hall.

As new Fellows arrive, we also take the time to thank those Fellows who have moved on to even bigger things:

Richard Teague moved to Massachusetts Institute of Technology recently to take up a faculty position in the Department of Earth, Atmospheric and Planetary Sciences. There, he will conduct his research on the earliest stages of planetary systems and planet formation.

Feng Long will depart in August 2022 to become the Sagan Fellow of the NASA Hubble Fellowship Program hosted at the University of Arizona. She will continue using sub-millimeter interferometers to pursue her research on protoplanetary disks and planet formation.

John Garrett departs in July 2022 after 3 years of post-doctoral fellowship in the Receiver Lab, during which he has successfully developed a prototype 345 GHz 2SB receiver for future wSMA upgrade. He will return to Canada and pursue a new career in quantum computing.

We wish all our current and former Fellowship holders continued success!

A list of current and former SMA Fellows is provided at:

<https://pweb.cfa.harvard.edu/opportunities/fellowships-visiting-scientist-positions/sma-postdoctoral-fellowships>

along with further information on the SMA Fellowship program and future SMA Fellowship opportunities.

Qizhou Zhang
Chair, SMA Fellowship Selection Committee

CALL FOR STANDARD OBSERVING PROPOSALS - 2022B SEMESTER

We wish to draw your attention to the next Call for Standard Observing Proposals for observations with the Submillimeter Array (SMA). This call is for the 2022B semester with observing period **08 December 2022 – 22 May 2023**.

Standard Observing Proposals Submission deadline: **Thursday, 22 September 2022 20:00 UTC**

The full Call for Proposals, with details on time available and the proposal process, will be available by August 21 at the SMA Observer Center (SMAOC) at <http://sma1.sma.hawaii.edu/call.html>.

Details on the SMA capabilities and status can be found at <http://sma1.sma.hawaii.edu/status.html>; proposal creation and submission is also done through the SMAOC at <http://sma1.sma.hawaii.edu/proposing.html>. We are happy to answer any questions and provide assistance in proposal submission; simply email sma-propose@cfa.harvard.edu with any inquiries.

Sincerely,

Mark Gurwell
SAO Chair, SMA TAC

Hau-Yu (Baobab) Liu
ASIAA Chair, SMA TAC

PROPOSAL STATISTICS FOR 2022A

The three SMA partner institutions received a total of 65 proposals (SAO 48, ASIAA 13, UHawaii 4) requesting observing time in the 2022A semester. In the Call for Proposals for 2022A, SAO proposers were notified that a significant amount of time would be going toward the SMA Large Scale Program (PI: Jan Forbrich) during much of late August through September, to complete that project. The 65 proposals were divided among science categories as follows:

CATEGORY	PROPOSALS
high mass (OB) star formation, cores	16
local galaxies, starbursts, AGN	14
low/intermediate mass star formation, cores	8
submm/hi-z galaxies	7
GRB, SN, high energy	6
protoplanetary, transition, debris disks	6
evolved stars, AGB, PPN	3
solar system	3
other	2

TRACK ALLOCATIONS BY WEATHER REQUIREMENT AND CONFIGURATION:

To best accommodate the highest ranked programs from each of the partners, as well as the SAO Large Scale Program (PI: Jan Forbrich, requiring SUB), it was determined that the configuration schedule would be:

EXT >> COM >> SUB >> EXT >> VEX

PWV ¹	SAO	ASIAA	UH ²
< 4.0mm	20A + 37B	6A + 19B	0
< 2.5mm	17A + 23B	3A + 1B	12
< 1.0mm	0A + 0B	6A + 0B	0
Total	37A + 60B	15A + 20B	12

Configuration	SAO	ASIAA	UH ²
Subcompact	2A + 11B	1A + 2B	0
Compact	8A + 19B	1A + 7B	5
Extended	13A + 7B	12A + 2B	5
Very Extended	6A + 2B	0	0
Either	8A + 21B	1A + 9B	2
Total	37A + 60B	15A + 20B	12

(1) Precipitable water vapor required for the observations. (2) UH does not list As and Bs.

TOP-RANKED 2022A SEMESTER PROPOSALS

The following is the listing of all SAO, ASIAA, and UH proposals with at least one A-rank track allocation.

GRB, SN, HIGH ENERGY

- 2022A-A008 Yuji Urata, NCU: "Electro-magnetic wave candidate of IceCube Neutrino event"
2022A-S039 Kishalay De, MIT: "Search for molecular emission in an exceptional Galactic stellar merger candidate"

EVOLVED STARS, AGB, PPN

- 2022A-S032 Sofia Wallström, KU Leuven "The Nearby Evolved Stars Survey: Exploring the inner AGB wind"

HIGH MASS (OB) STAR FORMATION, CORES

- 2022A-A003 Seamus Clarke, ASIAA: "Linking the fragmentation of clumps to the relative importance of gravity, turbulence and magnetic fields on multiple scales"
2022A-A007 Han-Tsung Lee, ASIAA/NCU: "Probe the multiscale magnetic field toward the filamentary infrared dark cloud SDC18"
2022A-A010 Han-Tsung Lee, ASIAA/NCU: "Multiscale B-field and fragmentation evolution of SDC18"
2022A-H004 Adwin Boogert, IfA: "Resolving disks in the massive protostellar binary W3 IRS5"
2022A-S018 Qizhou Zhang, CfA: "What drives the mini starburst in Sgr B2?"
2022A-S026 Todd Hunter, NRAO: "Triggered follow-up of accretion outbursts in massive protostars"

LOCAL GALAXIES, STARBURSTS, AGN

- 2022A-S004 Gerrit Schellenberger, CfA: "Probing the high frequency variability of NGC5044: the key to AGN feedback"
2022A-S022 Eric Koch, CfA: "A resolved molecular gas survey of the edge-on galaxy NGC 891"
2022A-S023 Eric Koch, CfA: "Resolving the molecular gas fuelling IC 10's starburst on 2.5 pc scales"

LOW/INTERMEDIATE MASS STAR FORMATION, CORES

- 2022A-H001 Goran Sandell, IfA/UH: "Finishing up the SMA study of the R Mon/NGC2261 molecular outflow"
2022A-S007 Carlos Eduardo Muñoz-Romero, CfA: "Resolving the Chemical Evolution of Class 0/I Protostars in Perseus"
2022A-S008 Jennifer Bergner, University of Chicago: "Molecular mapping of the chemically rich outflow B1-a"

OTHER

- 2022A-H003 Jason Hinkle, IfA/UH: "Rainbow tide: multi-wavelength follow-up of tidal disruption events"

PROTOPLANETARY, TRANSITION, DEBRIS DISKS

- 2022A-A011 Chia-Ying Chung, ASIAA: "The evidence of smaller maximum grain sizes than we expected in protoplanetary disks"
2022A-S003 David Wilner, CfA: "An Imaging Survey of Forgotten Nearby Herbig Ae/Be Stars (redux)"
2022A-S011 Feng Long, CfA: "Mapping the Gas Environment of Heavily Veiled Young Stars"

SOLAR SYSTEM

- 2022A-A006 Wei-Ling Tseng, NTNU: "Monitoring Io's dynamical volcanic eruptions and their contributions to Jupiter's magnetosphere"
2022A-S031 Mark Gurwell, CfA: "Polarized Emission from the Surface of Mars"

SUBMM/HI-Z GALAXIES

- 2022A-H002 Lennox Cowie, IfA/UH: "Developing a sample of faint submm sources and determining their properties"
2022A-S014 Giovanni Fazio, CfA: "Understanding the Evolution of Obscured Activity Out to $z>3$ — An Initial Phase SMA Survey of Submillimeter Sources in the JWST Time Domain Field"

STANDARD PROJECTS OBSERVED DURING 2021B

SMA Semester 2021B encompassed the period Nov 12, 2021 through Jun 15, 2022. After the proposal deadline, it was determined that the array would need a 1 month science hiatus (in February 2022) to address critical software upgrades, much needed maintenance and performance adjustments on the transporter, and time to work on two antennas with backlogged hardware failures and maintenance issues. In order to best accommodate this schedule change we limited the configuration schedule to the compact array (before the hiatus) and the extended array (after the hiatus), and pushed the end of the semester into June, past the typical May 15 end of semester.

Listed below are all SMA standard and DDT projects that were at least partially completed during the SMA Semester 2021B.

EVOLVED STARS, AGB, PPN

2021B-S033 Manali Jeste, MPIfR: "Imaging HCN emission from the carbon-rich AGB stars CQ Pyx, CIT 6, and V Hya"

GALACTIC CENTER

2021B-S049 Garrett Karto Keating, CfA: "Polarimetric VLBI for the 2022 Event Horizon Telescope Campaign"

2021B-S051 Sara Issaoun, CfA: "Probing Black Hole Accretion Flows with Faraday Rotation"

GRB, SN, HIGH ENERGY

2021B-A010 Yuji Urata, NCU: "Jet Structures of Gamma-Ray Bursts"

2021B-H006 Jason Hinkle, IfA/UH: "Rainbow tide: multi-wavelength follow-up of tidal disruption events"

2021B-S013 Anna Ho, UC Berkeley: "The Landscape of Relativistic Stellar Explosions"

2021B-S071 Anna Ho, UC Berkeley: "Continued Monitoring of ToO AT2022cmc"

2021B-S073 Kishalay De, MIT: "Search for molecular emission in an exceptional Galactic stellar merger candidate"

HIGH MASS (OB) STAR FORMATION, CORES

2021B-S004 Qizhou Zhang, CfA: "Magnetic Fields and protocluster formation"

2021B-S032 Wenyu Jiao, Peking University: "Probing the Initial conditions of extremely cold and low luminosity-to-mass ratio high-mass starless clumps within 3.5 kpc"

LOCAL GALAXIES, STARBURSTS, AGN

2021B-A009 Bo-Yan Chen, ASIAA: "Variability Timescale of Low Luminosity AGN"

2021B-S002 Peter Breiding, Johns Hopkins University: "SMA observations of the hybrid morphology radio jet 4C +13.41"

2021B-S006 Belinda Wilkes, CfA: "Radio Jet - Molecular Gas Feedback in the Compact Steep Spectrum Radio Galaxy 3C303.1"

2021B-S007 Gerrit Schellenberger, CfA: "UNDERSTANDING THE TIME VARIABILITY OF THE AGN IN NGC 5044"

2021B-S028 Joseph Cairns, Imperial College London: "The Sub-Millimeter Polarisation Properties of Local ULIRGs"

2021B-S035 Mojegan Azadi, CfA: "The Emission Mechanisms in Radio Galaxies at the Cosmic Peak of Star Formation Activity"

2021B-S043 Steven Willner, CfA: "Disentangling radiating particle properties and jet physics from M87 multi-wavelength variability"

2021B-S045 Peter Breiding, Johns Hopkins University: "3C 222: Can a Young and Powerful Agn Jet Forge Stars?"

2021B-S053 Venkatesh Ramakrishnan, University of Concepcion: "Polarimetric monitoring of the flaring blazar 1156+295"

2021B-S056 Mojegan Azadi, CfA: "Towards Understanding the Nature of the Youngest Gamma-Ray Emitting Radio Galaxies"

2021B-S066 Deanne Fisher, Swinburne University: "Testing Feedback Theory in Starbursting Disk Galaxies - Extended Tracks"

2021B-S067 Eric Koch, CfA: "Ay191 project: The resolved molecular gas in a nascent tidal dwarf galaxy"

2021B-S069 Venkatesh Ramakrishnan, University of Concepcion: "Probing the magnetic field structure at the base of the jet in 1156+295"

LOW/INTERMEDIATE MASS STAR FORMATION, CORES

- 2021B-A004 Dipen Sahu, ASIAA: "Stability of centrally dense prestellar cores at a scale of 2000 AU"
- 2021B-A005 Naomi Hirano, ASIAA: "Magnetic fields in the central regions of prestellar cores"
- 2021B-S029 Leticia Virginia Ferrero, Observatorio Astronómico de Córdoba: "Revealing the disk and the HH 31 jet/outflow, associated with IRAS 04248+2612, at small scales"
- 2021B-S034 Jennifer Bergner, University of Chicago: "Molecular mapping of the chemically rich outflow B1-a"
- 2021B-S037 Andrew Burkhardt, Wellesley College: "Resolving the Redshifted Outflow in the New Chemically-Active Outflow HH114: Is There a Precessing Jet, Episodic Ejection(s), or Both?"
- 2021B-S047 Josep Miquel Girart, CSIC-IEEC: "Molecular inventory of HH2"

PROTOPLANETARY, TRANSITION, DEBRIS DISKS

- 2021B-A003 Chia-Ying Chung, ASIAA: "A statistical study to constrain grain growth efficiency in protoplanetary disks"
- 2021B-A011 Chia-Ying Chung, ASIAA: "A statistical study to constrain grain growth efficiency in protoplanetary disks"
- 2021B-H002 Suchitra Narayanan, IfA/UH: "Search for sulfur organics in embedded disks in the Taurus molecular region"
- 2021B-H003 Jonathan Williams, IfA/UH: "Do disks clear out gradually or suddenly?"
- 2021B-S001 Richard Teague, CfA: "Is the Magneto-Rotational Instability Driving Protoplanetary Disk Evolution?"
- 2021B-S012 Sean Andrews, CfA: "Disk Evolution using the ""Distributed"" Taurus Population"
- 2021B-S014 Joshua Lovell, IfA/Cambridge: "Protoplanetary disc dissipation in Taurus: is dispersal rapid or gradual?"
- 2021B-S017 Feng Long, CfA: "Mapping the Gas Environment of Heavily Veiled Young Stars"
- 2021B-S021 Lucas Stapper, Leiden Observatory: "Chemistry in the UV-exposed disk of the AK Sco Herbig binary"

SOLAR SYSTEM

- 2021B-S054 Nathan Roth, NASA GSFC: "A Search for Distributed Sources at Small Heliocentric Distance in Comets C/2021 A1 (Leonard) and C/2021 O3 (PanSTARRS)"

SUBMM/HI-Z GALAXIES

- 2021B-A008 Zhen-Kai Gao, ASIAA: "SMA STUDIES IV: SCUBA-2 450 μ m Close Pairs"
- 2021B-A015 Ekaterina Koptelova, ASIAA: "Submm-continuum observation of the most distant BL Lacertae candidate FIRSTJ0849+29"
- 2021B-H001 Lennox Cowie, IfA/UH: "A uniquely massively star-forming protocluster at $z=3.15$ in the GOODS-N"
- 2021B-S010 Emily Moravec, NRAO: "Investigating Radio Active Galactic Nuclei and Their Host Galaxies in Merging Galaxy Clusters at $z\sim 1$ "
- 2021B-S011 Kevin Harrington, ESO-Chile: "Sub-kpc Imaging of the Multi-Phase ISM in Dusty Starbursts at $z=3$ "
- 2021B-S072 Steven Willner, CfA: "Two Very Bright 850 μ m Sources in a JWST GTO Field"

RECENT PUBLICATIONS

TITLE: Remarkable Correspondence of the Sagittarius A* Submillimeter Variability with a Stellar-wind-fed Accretion Flow Model
AUTHOR: Murchikova, L., White, C. J., Ressler, S. M.
PUBLICATION: *The Astrophysical Journal*, 932, L21
PUBLICATION DATE: 06/2022
ABSTRACT: <https://ui.adsabs.harvard.edu/abs/2022ApJ...932L..21M>
DOI: 10.3847/2041-8213/ac75c3

TITLE: Hard X-Ray Emission in Centaurus A
AUTHOR: Rani, B., Mundo, S. A., Mushotzky, R., Lien, A. Y., Gurwell, M. A., Kim, J. Y.
PUBLICATION: *The Astrophysical Journal*, 932, 104
PUBLICATION DATE: 06/2022
ABSTRACT: <https://ui.adsabs.harvard.edu/abs/2022ApJ...932..104R>
DOI: 10.3847/1538-4357/ac6fd4

TITLE: Jet kinematics in the transversely stratified jet of 3C 84 A two-decade overview
AUTHOR: Paraschos, G. F., Krichbaum, T. P., Kim, J.-Y., Hodgson, J. A., Oh, J., Ros, E., Zensus, J. A., Marscher, A. P., Jorstad, S. G., Gurwell, M. A., Lähteenmäki, A., Tornikoski, M., Kiehlmann, S., Readhead, A. C. S.
PUBLICATION: *arXiv e-prints*, [arXiv:2205.10281](https://arxiv.org/abs/2205.10281)
PUBLICATION DATE: 05/2022
ABSTRACT: <https://ui.adsabs.harvard.edu/abs/2022arXiv220510281P>
DOI:

TITLE: The methanol emission in the J1 - J0 A++ line series as a tracer of specific physical conditions in high-mass star-forming regions
AUTHOR: Saliı̇, S. V., Zinchenko, I. I., Liu, S.-Y., Sobolev, A. M., Aberfelds, A., Su, Y.-N.
PUBLICATION: *Monthly Notices of the Royal Astronomical Society*, 512, 3215-3229
PUBLICATION DATE: 05/2022
ABSTRACT: <https://ui.adsabs.harvard.edu/abs/2022MNRAS.512.3215S>
DOI: 10.1093/mnras/stac739

TITLE: Gas Disk Sizes from CO Line Observations: A Test of Angular Momentum Evolution
AUTHOR: Long, F., Andrews, S. M., Rosotti, G., Harsono, D., Pinilla, P., Wilner, D. J., Öberg, K. I., Teague, R., Trapman, L., Tabone, B.
PUBLICATION: *The Astrophysical Journal*, 931, 6
PUBLICATION DATE: 05/2022
ABSTRACT: <https://ui.adsabs.harvard.edu/abs/2022ApJ...931....6L>
DOI: 10.3847/1538-4357/ac634e

TITLE: Characterizing and Mitigating Intraday Variability: Reconstructing Source Structure in Accreting Black Holes with mm-VLBI

AUTHOR: Broderick, A. E., Gold, R., Georgiev, B., Pesce, D. W., Tiede, P., Ni, C., Moriyama, K., Akiyama, K., Alberdi, A., Alef, W., Algaba, J. C., Anantua, R., Asada, K., Azulay, R., Bach, U., Baczkó, A.-K., Ball, D., Baloković, M., Barrett, J., Bauböck, M., Benson, B. A., Bintley, D., Blackburn, L., Blundell, R., Bouman, K. L., Bower, G. C., Boyce, H., Bremer, M., Brinkerink, C. D., Brissenden, R., Britzen, S., Brogiere, D., Bronzwaer, T., Bustamante, S., Byun, D.-Y., Carlstrom, J. E., Ceccobello, C., Chael, A., Chan, C.-kwan., Chatterjee, K., Chatterjee, S., Chen, M.-T., Chen, Y., Cheng, X., Cho, I., Christian, P., Conroy, N. S., Conway, J. E., Cordes, J. M., Crawford, T. M., Crew, G. B., Cruz-Osorio, A., Cui, Y., Davelaar, J., De Laurentis, M., Deane, R., Dempsey, J., Desvignes, G., Dexter, J., Dhruv, V., Doeleman, S. S., Dougal, S., Dzib, S. A., Eatough, R. P., Emami, R., Falcke, H., Farah, J., Fish, V. L., Fomalont, E., Ford, H. A., Fraga-Encinas, R., Freeman, W. T., Friberg, P., Fromm, C. M., Fuentes, A., Galison, P., Gammie, C. F., García, R., Gentaz, O., Goddi, C., Gómez-Ruiz, A. I., Gómez, J. L., Gu, M., Gurwell, M., Hada, K., Haggard, D., Haworth, K., Hecht, M. H., Hesper, R., Heumann, D., Ho, L. C., Ho, P., Honma, M., Huang, C.-W. L., Huang, L., Hughes, D. H., Ikeda, S., Impellizzeri, C. M. V., Inoue, M., Issaoun, S., James, D. J., Jannuzi, B. T., Janssen, M., Jeter, B., Jiang, W., Jiménez-Rosales, A., Johnson, M. D., Jorstad, S., Joshi, A. V., Jung, T., Karami, M., Karuppusamy, R., Kawashima, T., Keating, G. K., Kettenis, M., Kim, D.-J., Kim, J.-Y., Kim, J., Kim, J., Kino, M., Koay, J. Y., Kocherlakota, P., Kofuji, Y., Koch, P. M., Koyama, S., Kramer, C., Kramer, M., Krichbaum, T. P., Kuo, C.-Y., La Bella, N., Lauer, T. R., Lee, D., Lee, S.-S., Leung, P. K., Levis, A., Li, Z., Lico, R., Lindahl, G., Lindqvist, M., Lisakov, M., Liu, J., Liu, K., Liuzzo, E., Lo, W.-P., Lobanov, A. P., Loinard, L., Lonsdale, C. J., Lu, R.-S., Mao, J., Marchili, N., Markoff, S., Marrone, D. P., Marscher, A. P., Martí-Vidal, I., Matsushita, S., Matthews, L. D., Menten, K. M., Michalik, D., Mizuno, I., Mizuno, Y., Moran, J. M., Moscibrodzka, M., Müller, C., Mus, A., Musoke, G., Myserlis, I., Nadolski, A., Nagai, H., Nagar, N. M., Nakamura, M., Narayan, R., Narayanan, G., Natarajan, I., Nathanail, A., Navarro Fuentes, S., Neilsen, J., Neri, R., Noutsos, A., Nowak, M. A., Oh, J., Okino, H., Olivares, H., Ortiz-León, G. N., Oyama, T., Palumbo, D. C. M., Paraschos, G. F., Park, J., Parsons, H., Patel, N., Pen, U.-L., Piétu, V., Plambeck, R., PopStefanija, A., Porth, O., Pötzel, F. M., Prather, B., Preciado-López, J. A., Pu, H.-Y., Ramakrishnan, V., Rao, R., Rawlings, M. G., Raymond, A. W., Rezzolla, L., Ricarte, A., Ripperda, B., Roelofs, F., Rogers, A., Ros, E., Romero-Cañizales, C., Roshanineshat, A., Rottmann, H., Roy, A. L., Ruiz, I., Ruszczyk, C., Rygl, K. L. J., Sánchez, S., Sánchez-Argüelles, D., Sánchez-Portal, M., Sasada, M., Satapathy, K., Savolainen, T., Schloerb, F. P., Schonfeld, J., Schuster, K.-F., Shao, L., Shen, Z., Small, D., Sohn, B. W., SooHoo, J., Souccar, K., Sun, H., Tazaki, F., Tetarenko, A. J., Tilanus, R. P. J., Titus, M., Torne, P., Traianou, E., Trent, T., Trippe, S., Turk, M., van Bemmell, I., van Langevelde, H. J., van Rossum, D. R., Vos, J., Wagner, J., Ward-Thompson, D., Wardle, J., Weintroub, J., Wex, N., Wharton, R., Wielgus, M., Wiik, K., Witzel, G., Wondrak, M. F., Wong, G. N., Wu, Q., Yamaguchi, P., Yoon, D., Young, A., Young, K., Younsi, Z., Yuan, F., Yuan, Y.-F., Zensus, J. A., Zhao, G.-Y., Zhang, S., Zhao, S.-S.

PUBLICATION: *The Astrophysical Journal*, 930, L21

PUBLICATION DATE: 05/2022

ABSTRACT: <https://ui.adsabs.harvard.edu/abs/2022ApJ...930L..21B>

DOI: 10.3847/2041-8213/ac6584

TITLE: A Universal Power-law Prescription for Variability from Synthetic Images of Black Hole Accretion Flows

AUTHOR: Georgiev, B., Pesce, D. W., Broderick, A. E., Wong, G. N., Dhruv, V., Wielgus, M., Gammie, C. F., Chan, C.-kwan., Chatterjee, K., Emami, R., Mizuno, Y., Gold, R., Fromm, C. M., Ricarte, A., Yoon, D., Joshi, A. V., Prather, B., Cruz-Osorio, A., Johnson, M. D., Porth, O., Olivares, H., Younsi, Z., Rezzolla, L., Vos, J., Qiu, R., Nathanail, A., Narayan, R., Chael, A., Anantua, R., Moscibrodzka, M., Akiyama, K., Alberdi, A., Alef, W., Algaba, J. C., Asada, K., Azulay, R., Bach, U., Baczkó, A.-K., Ball, D., Baloković, M., Barrett, J., Bauböck, M., Benson, B. A., Bintley, D., Blackburn, L., Blundell, R., Bouman, K. L., Bower, G. C., Boyce, H., Bremer, M., Brinkerink, C. D., Brissenden, R., Britzen, S., Brogiere, D., Bronzwaer, T., Bustamante, S., Byun, D.-Y., Carlstrom, J. E., Ceccobello, C., Chatterjee, S., Chen, M.-T., Chen, Y., Cheng, X., Cho, I., Christian, P., Conroy, N. S., Conway, J. E., Cordes, J. M., Crawford, T. M., Crew, G. B., Cui, Y., Davelaar, J., De Laurentis, M., Deane, R., Dempsey, J., Desvignes, G., Dexter, J., Doeleman, S. S., Dougal, S., Dzib, S. A., Eatough, R. P., Falcke, H., Farah, J., Fish, V. L., Fomalont, E., Ford, H. A., Fraga-Encinas, R., Freeman, W. T., Friberg, P., Fuentes, A., Galison, P., García, R., Gentaz, O., Goddi, C., Gómez-Ruiz, A. I., Gómez, J. L., Gu, M., Gurwell, M., Hada, K., Haggard, D., Haworth, K., Hecht, M. H., Hesper, R., Heumann, D., Ho, L. C., Ho, P., Honma, M., Huang, C.-W. L., Huang, L., Hughes, D. H., Ikeda, S., Impellizzeri, C. M. V., Inoue, M., Issaoun, S., James, D. J., Jannuzi, B. T., Janssen, M., Jeter, B., Jiang, W., Jiménez-Rosales, A., Jorstad, S., Jung, T., Karami, M., Karuppusamy, R., Kawashima, T., Keating, G. K., Kettenis, M., Kim, D.-J., Kim, J.-Y., Kim, J., Kim, J., Kino, M., Koay, J. Y., Kocherlakota, P., Kofuji, Y., Koch, P. M., Koyama, S., Kramer, C., Kramer,

M., Krichbaum, T. P., Kuo, C.-Y., La Bella, N., Lauer, T. R., Lee, D., Lee, S.-S., Lehner, L., Leung, P. K., Levis, A., Li, Z., Lico, R., Lindahl, G., Lindqvist, M., Lisakov, M., Liu, J., Liu, K., Liuzzo, E., Lo, W.-P., Lobanov, A. P., Loinard, L., Lonsdale, C. J., Lu, R.-S., Mao, J., Marchili, N., Markoff, S., Marrone, D. P., Marscher, A. P., Martí-Vidal, I., Matsushita, S., Matthews, L. D., Menten, K. M., Michalik, D., Mizuno, I., Moran, J. M., Moriyama, K., Müller, C., Mus, A., Musoke, G., Myserlis, I., Nadolski, A., Nagai, H., Nagar, N. M., Nakamura, M., Narayanan, G., Natarajan, I., Navarro Fuentes, S., Neilsen, J., Neri, R., Ni, C., Noutsos, A., Nowak, M. A., Oh, J., Okino, H., Ortiz-León, G. N., Oyama, T., Palumbo, D. C. M., Paraschos, G. F., Park, J., Parsons, H., Patel, N., Pen, U.-L., Piétu, V., Plambeck, R., PopStefanija, A., Pötzl, F. M., Preciado-López, J. A., Pu, H.-Y., Ramakrishnan, V., Rao, R., Rawlings, M. G., Raymond, A. W., Ripperda, B., Roelofs, F., Rogers, A., Ros, E., Romero-Cañizales, C., Roshanineshat, A., Rottmann, H., Roy, A. L., Ruiz, I., Ruszczyk, C., Rygl, K. L. J., Sánchez, S., Sánchez-Argüelles, D., Sánchez-Portal, M., Sasada, M., Satopathy, K., Savolainen, T., Schloerb, F. P., Schonfeld, J., Schuster, K.-F., Shao, L., Shen, Z., Small, D., Sohn, B. W., SooHoo, J., Souccar, K., Sun, H., Tazaki, F., Tetarenko, A. J., Tiede, P., Tilanus, R. P. J., Titus, M., Torne, P., Traianou, E., Trent, T., Trippe, S., Turk, M., van Bemmell, I., van Langevelde, H. J., van Rossum, D. R., Wagner, J., Ward-Thompson, D., Wardle, J., Weintroub, J., Wex, N., Wharton, R., Wiik, K., Witzel, G., Wondrak, M. F., Wu, Q., Yamaguchi, P., Young, A., Young, K., Yuan, F., Yuan, Y.-F., Zensus, J. A., Zhang, S., Zhao, G.-Y., Zhao, S.-S.

PUBLICATION: *The Astrophysical Journal*, 930, L20

PUBLICATION DATE: 05/2022

ABSTRACT: <https://ui.adsabs.harvard.edu/abs/2022ApJ...930L..20G>

DOI: 10.3847/2041-8213/ac65eb

TITLE: Millimeter Light Curves of Sagittarius A* Observed during the 2017 Event Horizon Telescope Campaign

AUTHOR: Wielgus, M., Marchili, N., Martí-Vidal, I., Keating, G. K., Ramakrishnan, V., Tiede, P., Fomalont, E., Issaoun, S., Neilsen, J., Nowak, M. A., Blackburn, L., Gammie, C. F., Goddi, C., Haggard, D., Lee, D., Moscibrodzka, M., Tetarenko, A. J., Bower, G. C., Chan, C.-kwan, Chatterjee, K., Chesler, P. M., Dexter, J., Doeleman, S. S., Georgiev, B., Gurwell, M., Johnson, M. D., Marrone, D. P., Mus, A., Psaltis, D., Ripperda, B., Witzel, G., Akiyama, K., Alberdi, A., Alef, W., Algaba, J. C., Anantua, R., Asada, K., Azulay, R., Bach, U., Baczko, A.-K., Ball, D., Baloković, M., Barrett, J., Bauböck, M., Benson, B. A., Bintley, D., Blundell, R., Boland, W., Bouman, K. L., Boyce, H., Bremer, M., Brinkerink, C. D., Brissenden, R., Britzen, S., Broderick, A. E., Brogiere, D., Bronzwaer, T., Bustamante, S., Byun, D.-Y., Carlstrom, J. E., Ceccobello, C., Chael, A., Chatterjee, S., Chen, M.-T., Chen, Y., Cho, I., Christian, P., Conroy, N. S., Conway, J. E., Cordes, J. M., Crawford, T. M., Crew, G. B., Cruz-Osorio, A., Cui, Y., Davelaar, J., De Laurentis, M., Deane, R., Dempsey, J., Desvignes, G., Dhruv, V., Dzib, S. A., Eatough, R. P., Emami, R., Falcke, H., Farah, J., Fish, V. L., Ford, H. A., Fraga-Encinas, R., Freeman, W. T., Friberg, P., Fromm, C. M., Fuentes, A., Galison, P., García, R., Gentaz, O., Gold, R., Gómez-Ruiz, A. I., Gómez, J. L., Gu, M., Hada, K., Haworth, K., Hecht, M. H., Hesper, R., Ho, L. C., Ho, P., Honma, M., Huang, C.-W. L., Huang, L., Hughes, D. H., Ikeda, S., Impellizzeri, C. M. V., Inoue, M., James, D. J., Jannuzi, B. T., Janssen, M., Jeter, B., Jiang, W., Jiménez-Rosales, A., Jorstad, S., Joshi, A. V., Jung, T., Karami, M., Karuppusamy, R., Kawashima, T., Kettenis, M., Kim, D.-J., Kim, J.-Y., Kim, J., Kim, J., Kino, M., Koay, J. Y., Kocherlakota, P., Kofuji, Y., Koch, P. M., Koyama, S., Kramer, C., Kramer, M., Krichbaum, T. P., Kuo, C.-Y., La Bella, N., Lauer, T. R., Lee, S.-S., Leung, P. K., Levis, A., Li, Z., Lico, R., Lindahl, G., Lindqvist, M., Lisakov, M., Liu, J., Liu, K., Liuzzo, E., Lo, W.-P., Lobanov, A. P., Loinard, L., Lonsdale, C., Lu, R.-S., Mao, J., Markoff, S., Marscher, A. P., Matsushita, S., Matthews, L. D., Medeiros, L., Menten, K. M., Michalik, D., Mizuno, I., Mizuno, Y., Moran, J. M., Moriyama, K., Müller, C., Musoke, G., Myserlis, I., Nadolski, A., Nagai, H., Nagar, N. M., Nakamura, M., Narayan, R., Narayanan, G., Natarajan, I., Nathanail, A., Navarro Fuentes, S., Neri, R., Ni, C., Noutsos, A., Oh, J., Okino, H., Olivares, H., Ortiz-León, G. N., Oyama, T., Özel, F., Palumbo, D. C. M., Paraschos, G. F., Park, J., Parsons, H., Patel, N., Pen, U.-L., Pesce, D. W., Piétu, V., Plambeck, R., PopStefanija, A., Porth, O., Pötzl, F. M., Prather, B., Preciado-López, J. A., Pu, H.-Y., Rao, R., Rawlings, M. G., Raymond, A. W., Rezzolla, L., Ricarte, A., Roelofs, F., Rogers, A., Ros, E., Romero-Canizales, C., Roshanineshat, A., Rottmann, H., Roy, A. L., Ruiz, I., Ruszczyk, C., Rygl, K. L. J., Sánchez, S., Sánchez-Argüelles, D., Sánchez-Portal, M., Sasada, M., Satopathy, K., Savolainen, T., Schloerb, F. P., Schuster, K.-F., Shao, L., Shen, Z., Small, D., Won Sohn, B., SooHoo, J., Souccar, K., Sun, H., Tazaki, F., Tilanus, R. P. J., Titus, M., Torne, P., Traianou, E., Trent, T., Trippe, S., van Bemmell, I., van Langevelde, H. J., van Rossum, D. R., Vos, J., Wagner, J., Ward-Thompson, D., Wardle, J., Weintroub, J., Wex, N., Wharton, R., Wiik, K., Wondrak, M. F., Wong, G. N., Wu, Q., Yamaguchi, P., Yoon, D., Young, A., Young, K., Younsi, Z., Yuan, F., Yuan, Y.-F., Zensus, J. A., Zhang, S., Zhao, G.-Y., Zhao, S.-S.

PUBLICATION: *The Astrophysical Journal*, 930, L19

PUBLICATION DATE: 05/2022

ABSTRACT: <https://ui.adsabs.harvard.edu/abs/2022ApJ...930L..19W>

DOI: 10.3847/2041-8213/ac6428

TITLE: Selective Dynamical Imaging of Interferometric Data

AUTHOR: Farah, J., Galison, P., Akiyama, K., Bouman, K. L., Bower, G. C., Chael, A., Fuentes, A., Gómez, J. L., Honma, M., Johnson, M. D., Kofuji, Y., Marrone, D. P., Moriyama, K., Narayan, R., Pesce, D. W., Tiede, P., Wielgus, M., Zhao, G.-Y., Alberdi, A., Alef, W., Algaba, J. C., Anantua, R., Asada, K., Azulay, R., Baczko, A.-K., Ball, D., Baloković, M., Barrett, J., Benson, B. A., Bintley, D., Blackburn, L., Blundell, R., Boland, W., Boyce, H., Bremer, M., Brinkerink, C. D., Brissenden, R., Britzen, S., Broderick, A. E., Brogiere, D., Bronzwaer, T., Bustamante, S., Byun, D.-Y., Carlstrom, J. E., Chan, C.-kwan., Chatterjee, K., Chatterjee, S., Chen, M.-T., Chen, Y., Cho, I., Christian, P., Conway, J. E., Cordes, J. M., Crawford, T. M., Crew, G. B., Cruz-Osorio, A., Cui, Y., Davelaar, J., De Laurentis, M., Deane, R., Dempsey, J., Desvignes, G., Doeleman, S. S., Eatough, R. P., Falcke, H., Fish, V. L., Fomalont, E., Ford, H. A., Fraga-Encinas, R., Friberg, P., Fromm, C. M., Gammie, C. F., Garca, R., Gentaz, O., Goddi, C., Gold, R., Gómez-Ruiz, A. I., Gu, M., Gurwell, M., Hada, K., Haggard, D., Hecht, M. H., Hesper, R., Ho, L. C., Ho, P., Huang, C.-W. L., Huang, L., Hughes, D. H., Ikeda, S., Inoue, M., Issaoun, S., James, D. J., Jannuzi, B. T., Janssen, M., Jeter, B., Jiang, W., Jimenez-Rosales, A., Jorstad, S., Jung, T., Karami, M., Karuppusamy, R., Kawashima, T., Keating, G. K., Kettenis, M., Kim, D.-J., Kim, J.-Y., Kim, J., Kim, J., Kino, M., Koay, J. Y., Koch, P. M., Koyama, S., Kramer, C., Kramer, M., Krichbaum, T. P., Kuo, C.-Y., Lauer, T. R., Lee, S.-S., Levis, A., Li, Y.-R., Li, Z., Lico, R., Lindahl, G., Lindqvist, M., Liu, J., Liu, K., Liuzzo, E., Lo, W.-P., Lobanov, A. P., Loinard, L., Lonsdale, C., Lu, R.-S., MacDonald, N. R., Mao, J., Marchili, N., Markoff, S., Marscher, A. P., Martí-Vidal, I., Matsushita, S., Matthews, L. D., Medeiros, L., Menten, K. M., Mizuno, I., Mizuno, Y., Moran, J. M., Moscibrodzka, M., Müller, C., Mejas, A. M., Musoke, G., Nagai, H., Nagar, N. M., Nakamura, M., Narayanan, G., Natarajan, I., Nathanail, A., Neilsen, J., Neri, R., Ni, C., Noutsos, A., Nowak, M. A., Okino, H., Olivares, H., Ortiz-León, G. N., Oyama, T., zel, F., Palumbo, D. C. M., Park, J., Patel, N., Pen, U.-L., Piétu, V., Plambeck, R., PopStefanija, A., Porth, O., Pötzl, F. M., Prather, B., Preciado-López, J. A., Psaltis, D., Pu, H.-Y., Ramakrishnan, V., Rao, R., Rawlings, M. G., Raymond, A. W., Rezzolla, L., Ripperda, B., Roelofs, F., Rogers, A., Ros, E., Rose, M., Roshanineshat, A., Rottmann, H., Roy, A. L., Ruszczyk, C., Rygl, K. L. J., Sánchez, S., Sánchez-Arguelles, D., Sasada, M., Savolainen, T., Schloerb, F. P., Schuster, K.-F., Shao, L., Shen, Z., Small, D., Sohn, B. W., SooHoo, J., Sun, H., Tazaki, F., Tetarenko, A. J., Tilanus, R. P. J., Titus, M., Toma, K., Torne, P., Traianou, E., Trent, T., Trippe, S., van Bemmell, I., van Langevelde, H. J., van Rossum, D. R., Wagner, J., Ward-Thompson, D., Wardle, J., Weintraub, J., Wex, N., Wharton, R., Wiik, K., Wong, G. N., Wu, Q., Yoon, D., Young, A., Young, K., Younsi, Z., Yuan, F., Yuan, Y.-F., Zensus, J. A., Zhao, S.-S., Event Horizon Telescope Collaboration

PUBLICATION: *The Astrophysical Journal*, 930, L18

PUBLICATION DATE: 05/2022

ABSTRACT: <https://ui.adsabs.harvard.edu/abs/2022ApJ...930L..18F>

DOI: 10.3847/2041-8213/ac6615

TITLE: First Sagittarius A* Event Horizon Telescope Results. VI. Testing the Black Hole Metric

AUTHOR: Akiyama, K., Alberdi, A., Alef, W., Algaba, J. C., Anantua, R., Asada, K., Azulay, R., Bach, U., Baczko, A.-K., Ball, D., Baloković, M., Barrett, J., Bauböck, M., Benson, B. A., Bintley, D., Blackburn, L., Blundell, R., Bouman, K. L., Bower, G. C., Boyce, H., Bremer, M., Brinkerink, C. D., Brissenden, R., Britzen, S., Broderick, A. E., Brogiere, D., Bronzwaer, T., Bustamante, S., Byun, D.-Y., Carlstrom, J. E., Ceccobello, C., Chael, A., Chan, C.-kwan., Chatterjee, K., Chatterjee, S., Chen, M.-T., Chen, Y., Cheng, X., Cho, I., Christian, P., Conroy, N. S., Conway, J. E., Cordes, J. M., Crawford, T. M., Crew, G. B., Cruz-Osorio, A., Cui, Y., Davelaar, J., De Laurentis, M., Deane, R., Dempsey, J., Desvignes, G., Dexter, J., Dhruv, V., Doeleman, S. S., Dougal, S., Dzib, S. A., Eatough, R. P., Emami, R., Falcke, H., Farah, J., Fish, V. L., Fomalont, E., Ford, H. A., Fraga-Encinas, R., Freeman, W. T., Friberg, P., Fromm, C. M., Fuentes, A., Galison, P., Gammie, C. F., García, R., Gentaz, O., Georgiev, B., Goddi, C., Gold, R., Gómez-Ruiz, A. I., Gómez, J. L., Gu, M., Gurwell, M., Hada, K., Haggard, D., Haworth, K., Hecht, M. H., Hesper, R., Heumann, D., Ho, L. C., Ho, P., Honma, M., Huang, C.-W. L., Huang, L., Hughes, D. H., Ikeda, S., Impellizzeri, C. M. V., Inoue, M., Issaoun, S., James, D. J., Jannuzi, B. T., Janssen, M., Jeter, B., Jiang, W., Jiménez-Rosales, A., Johnson, M. D., Jorstad, S., Joshi, A. V., Jung, T., Karami, M., Karuppusamy, R., Kawashima, T., Keating, G. K., Kettenis, M., Kim, D.-J., Kim, J.-Y., Kim, J., Kim, J., Kino, M., Koay, J. Y., Kocherlakota, P., Kofuji, Y., Koch, P. M., Koyama, S., Kramer, C., Kramer, M., Krichbaum, T. P., Kuo, C.-Y., La Bella, N., Lauer, T. R., Lee, D., Lee, S.-S., Leung, P. K., Levis, A., Li, Z., Lico, R., Lindahl, G., Lindqvist, M., Lisakov, M., Liu, J., Liu, K., Liuzzo, E., Lo, W.-P., Lobanov, A. P., Loinard, L., Lonsdale, C. J., Lu, R.-S., Mao, J., Marchili, N., Markoff, S., Marrone, D. P., Marscher, A. P., Martí-Vidal, I., Matsushita, S., Matthews, L. D., Medeiros, L., Menten, K. M., Michalik, D., Mizuno, I., Mizuno, Y., Moran, J. M., Moriyama, K., Moscibrodzka, M., Müller, C., Mus, A., Musoke, G., Myserlis, I., Nadolski, A., Nagai, H., Nagar, N. M., Nakamura, M., Narayan, R., Narayanan, G., Natarajan, I., Nathanail, A., Navarro Fuentes, S., Neilsen, J., Neri, R., Ni, C., Noutsos, A.,

Nowak, M. A., Oh, J., Okino, H., Olivares, H., Ortiz-León, G. N., Oyama, T., Özel, F., Palumbo, D. C. M., Paraschos, G. F., Park, J., Parsons, H., Patel, N., Pen, U.-L., Pesce, D. W., Piétu, V., Plambeck, R., PopStefanija, A., Porth, O., Pötzl, F. M., Prather, B., Preciado-López, J. A., Psaltis, D., Pu, H.-Y., Ramakrishnan, V., Rao, R., Rawlings, M. G., Raymond, A. W., Rezzolla, L., Ricarte, A., Ripperda, B., Roelofs, F., Rogers, A., Ros, E., Romero-Cañizales, C., Roshanineshat, A., Rottmann, H., Roy, A. L., Ruiz, I., Ruszczyk, C., Rygl, K. L. J., Sánchez, S., Sánchez-Argüelles, D., Sánchez-Portal, M., Sasada, M., Satopathy, K., Savolainen, T., Schloerb, F. P., Schonfeld, J., Schuster, K.-F., Shao, L., Shen, Z., Small, D., Sohn, B. W., SooHoo, J., Souccar, K., Sun, H., Tazaki, F., Tetarenko, A. J., Tiede, P., Tilanus, R. P. J., Titus, M., Torne, P., Traianou, E., Trent, T., Trippe, S., Turk, M., van Bemmell, I., van Langevelde, H. J., van Rossum, D. R., Vos, J., Wagner, J., Ward-Thompson, D., Wardle, J., Weintroub, J., Wex, N., Wharton, R., Wielgus, M., Wiik, K., Witzel, G., Wondrak, M. F., Wong, G. N., Wu, Q., Yamaguchi, P., Yoon, D., Young, A., Young, K., Younsi, Z., Yuan, F., Yuan, Y.-F., Zensus, J. A., Zhang, S., Zhao, G.-Y., Zhao, S.-S., EHT Collaboration

PUBLICATION: *The Astrophysical Journal*, 930, L17

PUBLICATION DATE: 05/2022

ABSTRACT: <https://ui.adsabs.harvard.edu/abs/2022ApJ...930L..17A>

DOI: 10.3847/2041-8213/ac6756

TITLE: First Sagittarius A* Event Horizon Telescope Results. V. Testing Astrophysical Models of the Galactic Center Black Hole

AUTHOR: Akiyama, K., Alberdi, A., Alef, W., Algaba, J. C., Anantua, R., Asada, K., Azulay, R., Bach, U., Baczko, A.-K., Ball, D., Baloković, M., Barrett, J., Bauböck, M., Benson, B. A., Bintley, D., Blackburn, L., Blundell, R., Bouman, K. L., Bower, G. C., Boyce, H., Bremer, M., Brinkerink, C. D., Brissenden, R., Britzen, S., Broderick, A. E., Brogiere, D., Bronzwaer, T., Bustamante, S., Byun, D.-Y., Carlstrom, J. E., Ceccobello, C., Chael, A., Chan, C.-kwan., Chatterjee, K., Chatterjee, S., Chen, M.-T., Chen, Y., Cheng, X., Cho, I., Christian, P., Conroy, N. S., Conway, J. E., Cordes, J. M., Crawford, T. M., Crew, G. B., Cruz-Osorio, A., Cui, Y., Davelaar, J., De Laurentis, M., Deane, R., Dempsey, J., Desvignes, G., Dexter, J., Dhruv, V., Doleman, S. S., Dougal, S., Dzib, S. A., Eatough, R. P., Emami, R., Falcke, H., Farah, J., Fish, V. L., Fomalont, E., Ford, H. A., Fraga-Encinas, R., Freeman, W. T., Friberg, P., Fromm, C. M., Fuentes, A., Galison, P., Gammie, C. F., García, R., Gentaz, O., Georgiev, B., Goddi, C., Gold, R., Gómez-Ruiz, A. I., Gómez, J. L., Gu, M., Gurwell, M., Hada, K., Haggard, D., Haworth, K., Hecht, M. H., Hesper, R., Heumann, D., Ho, L. C., Ho, P., Honma, M., Huang, C.-W. L., Huang, L., Hughes, D. H., Ikeda, S., Impellizzeri, C. M. V., Inoue, M., Issaoun, S., James, D. J., Jannuzi, B. T., Janssen, M., Jeter, B., Jiang, W., Jiménez-Rosales, A., Johnson, M. D., Jorstad, S., Joshi, A. V., Jung, T., Karami, M., Karuppusamy, R., Kawashima, T., Keating, G. K., Kettenis, M., Kim, D.-J., Kim, J.-Y., Kim, J., Kim, J., Kino, M., Koay, J. Y., Kocherlakota, P., Kofuji, Y., Koch, P. M., Koyama, S., Kramer, C., Kramer, M., Krichbaum, T. P., Kuo, C.-Y., La Bella, N., Lauer, T. R., Lee, D., Lee, S.-S., Leung, P. K., Levis, A., Li, Z., Lico, R., Lindahl, G., Lindqvist, M., Lisakov, M., Liu, J., Liu, K., Liuzzo, E., Lo, W.-P., Lobanov, A. P., Loinard, L., Lonsdale, C. J., Lu, R.-S., Mao, J., Marchili, N., Markoff, S., Marrone, D. P., Marscher, A. P., Martí-Vidal, I., Matsushita, S., Matthews, L. D., Medeiros, L., Menten, K. M., Michalik, D., Mizuno, I., Mizuno, Y., Moran, J. M., Moriyama, K., Moscibrodzka, M., Müller, C., Mus, A., Musoke, G., Myserlis, I., Nadolski, A., Nagai, H., Nagar, N. M., Nakamura, M., Narayan, R., Narayanan, G., Natarajan, I., Nathanail, A., Navarro Fuentes, S., Neilsen, J., Neri, R., Ni, C., Noutsos, A., Nowak, M. A., Oh, J., Okino, H., Olivares, H., Ortiz-León, G. N., Oyama, T., Özel, F., Palumbo, D. C. M., Paraschos, G. F., Park, J., Parsons, H., Patel, N., Pen, U.-L., Pesce, D. W., Piétu, V., Plambeck, R., PopStefanija, A., Porth, O., Pötzl, F. M., Prather, B., Preciado-López, J. A., Psaltis, D., Pu, H.-Y., Ramakrishnan, V., Rao, R., Rawlings, M. G., Raymond, A. W., Rezzolla, L., Ricarte, A., Ripperda, B., Roelofs, F., Rogers, A., Ros, E., Romero-Cañizales, C., Roshanineshat, A., Rottmann, H., Roy, A. L., Ruiz, I., Ruszczyk, C., Rygl, K. L. J., Sánchez, S., Sánchez-Argüelles, D., Sánchez-Portal, M., Sasada, M., Satopathy, K., Savolainen, T., Schloerb, F. P., Schonfeld, J., Schuster, K.-F., Shao, L., Shen, Z., Small, D., Sohn, B. W., SooHoo, J., Souccar, K., Sun, H., Tazaki, F., Tetarenko, A. J., Tiede, P., Tilanus, R. P. J., Titus, M., Torne, P., Traianou, E., Trent, T., Trippe, S., Turk, M., van Bemmell, I., van Langevelde, H. J., van Rossum, D. R., Vos, J., Wagner, J., Ward-Thompson, D., Wardle, J., Weintroub, J., Wex, N., Wharton, R., Wielgus, M., Wiik, K., Witzel, G., Wondrak, M. F., Wong, G. N., Wu, Q., Yamaguchi, P., Yoon, D., Young, A., Young, K., Younsi, Z., Yuan, F., Yuan, Y.-F., Zensus, J. A., Zhang, S., Zhao, G.-Y., Zhao, S.-S., Chan, T. L., Qiu, R., Ressler, S., White, C., EHT Collaboration

PUBLICATION: *The Astrophysical Journal*, 930, L16

PUBLICATION DATE: 05/2022

ABSTRACT: <https://ui.adsabs.harvard.edu/abs/2022ApJ...930L..16A>

DOI: 10.3847/2041-8213/ac6672

TITLE: First Sagittarius A* Event Horizon Telescope Results. IV. Variability, Morphology, and Black Hole Mass
AUTHOR: Akiyama, K., Alberdi, A., Alef, W., Algaba, J. C., Anantua, R., Asada, K., Azulay, R., Bach, U., Baczko, A.-K., Ball, D., Baloković, M., Barrett, J., Bauböck, M., Benson, B. A., Bintley, D., Blackburn, L., Blundell, R., Bouman, K. L., Bower, G. C., Boyce, H., Bremer, M., Brinkerink, C. D., Brissenden, R., Britzen, S., Broderick, A. E., Brogiere, D., Bronzwaer, T., Bustamante, S., Byun, D.-Y., Carlstrom, J. E., Ceccobello, C., Chael, A., Chan, C.-kwan., Chatterjee, K., Chatterjee, S., Chen, M.-T., Chen, Y., Cheng, X., Cho, I., Christian, P., Conroy, N. S., Conway, J. E., Cordes, J. M., Crawford, T. M., Crew, G. B., Cruz-Osorio, A., Cui, Y., Davelaar, J., De Laurentis, M., Deane, R., Dempsey, J., Desvignes, G., Dexter, J., Dhruv, V., Doleman, S. S., Dougal, S., Dzib, S. A., Eatough, R. P., Emami, R., Falcke, H., Farah, J., Fish, V. L., Fomalont, E., Ford, H. A., Fraga-Encinas, R., Freeman, W. T., Friberg, P., Fromm, C. M., Fuentes, A., Galison, P., Gammie, C. F., García, R., Gentaz, O., Georgiev, B., Goddi, C., Gold, R., Gómez-Ruiz, A. I., Gómez, J. L., Gu, M., Gurwell, M., Hada, K., Haggard, D., Haworth, K., Hecht, M. H., Hesper, R., Heumann, D., Ho, L. C., Ho, P., Honma, M., Huang, C.-W. L., Huang, L., Hughes, D. H., Ikeda, S., Impellizzeri, C. M. V., Inoue, M., Issaoun, S., James, D. J., Jannuzi, B. T., Janssen, M., Jeter, B., Jiang, W., Jiménez-Rosales, A., Johnson, M. D., Jorstad, S., Joshi, A. V., Jung, T., Karami, M., Karuppusamy, R., Kawashima, T., Keating, G. K., Kettenis, M., Kim, D.-J., Kim, J.-Y., Kim, J., Kim, J., Kino, M., Koay, J. Y., Kocherlakota, P., Kofuji, Y., Koch, P. M., Koyama, S., Kramer, C., Kramer, M., Krichbaum, T. P., Kuo, C.-Y., La Bella, N., Lauer, T. R., Lee, D., Lee, S.-S., Leung, P. K., Levis, A., Li, Z., Lico, R., Lindahl, G., Lindqvist, M., Lisakov, M., Liu, J., Liu, K., Liuzzo, E., Lo, W.-P., Lobanov, A. P., Loinard, L., Lonsdale, C. J., Lu, R.-S., Mao, J., Marchili, N., Markoff, S., Marrone, D. P., Marscher, A. P., Martí-Vidal, I., Matsushita, S., Matthews, L. D., Medeiros, L., Menten, K. M., Michalik, D., Mizuno, I., Mizuno, Y., Moran, J. M., Moriyama, K., Moscibrodzka, M., Müller, C., Mus, A., Musoke, G., Myserlis, I., Nadolski, A., Nagai, H., Nagar, N. M., Nakamura, M., Narayan, R., Narayanan, G., Natarajan, I., Nathanail, A., Navarro Fuentes, S., Neilsen, J., Neri, R., Ni, C., Noutsos, A., Nowak, M. A., Oh, J., Okino, H., Olivares, H., Ortiz-León, G. N., Oyama, T., Palumbo, D. C. M., Paraschos, G. F., Park, J., Parsons, H., Patel, N., Pen, U.-L., Pesce, D. W., Piétu, V., Plambeck, R., PopStefanija, A., Porth, O., Pötzl, F. M., Prather, B., Preciado-López, J. A., Pu, H.-Y., Ramakrishnan, V., Rao, R., Rawlings, M. G., Raymond, A. W., Rezzolla, L., Ricarte, A., Ripperda, B., Roelofs, F., Rogers, A., Ros, E., Romero-Cañizales, C., Roshanineshat, A., Rottmann, H., Roy, A. L., Ruiz, I., Ruszczyk, C., Rygl, K. L. J., Sánchez, S., Sánchez-Argüelles, D., Sánchez-Portal, M., Sasada, M., Satpathy, K., Savolainen, T., Schloerb, F. P., Schonfeld, J., Schuster, K.-F., Shao, L., Shen, Z., Small, D., Sohn, B. W., SooHoo, J., Souccar, K., Sun, H., Tazaki, F., Tetarenko, A. J., Tiede, P., Tilanus, R. P. J., Titus, M., Torne, P., Traianou, E., Trent, T., Trippe, S., Turk, M., van Bemmell, I., van Langevelde, H. J., van Rossum, D. R., Vos, J., Wagner, J., Ward-Thompson, D., Wardle, J., Weintroub, J., Wex, N., Wharton, R., Wielgus, M., Wiik, K., Witzel, G., Wondrak, M. F., Wong, G. N., Wu, Q., Yamaguchi, P., Yoon, D., Young, A., Young, K., Younsi, Z., Yuan, F., Yuan, Y.-F., Zensus, J. A., Zhang, S., Zhao, G.-Y., Zhao, S.-S., Chang, D. O., EHT Collaboration
PUBLICATION: *The Astrophysical Journal*, 930, L15
PUBLICATION DATE: 05/2022
ABSTRACT: <https://ui.adsabs.harvard.edu/abs/2022ApJ...930L..15A>
DOI: 10.3847/2041-8213/ac6736

TITLE: First Sagittarius A* Event Horizon Telescope Results. III. Imaging of the Galactic Center Supermassive Black Hole
AUTHOR: Akiyama, K., Alberdi, A., Alef, W., Algaba, J. C., Anantua, R., Asada, K., Azulay, R., Bach, U., Baczko, A.-K., Ball, D., Baloković, M., Barrett, J., Bauböck, M., Benson, B. A., Bintley, D., Blackburn, L., Blundell, R., Bouman, K. L., Bower, G. C., Boyce, H., Bremer, M., Brinkerink, C. D., Brissenden, R., Britzen, S., Broderick, A. E., Brogiere, D., Bronzwaer, T., Bustamante, S., Byun, D.-Y., Carlstrom, J. E., Ceccobello, C., Chael, A., Chan, C.-kwan., Chatterjee, K., Chatterjee, S., Chen, M.-T., Chen, Y., Cheng, X., Cho, I., Christian, P., Conroy, N. S., Conway, J. E., Cordes, J. M., Crawford, T. M., Crew, G. B., Cruz-Osorio, A., Cui, Y., Davelaar, J., De Laurentis, M., Deane, R., Dempsey, J., Desvignes, G., Dexter, J., Dhruv, V., Doleman, S. S., Dougal, S., Dzib, S. A., Eatough, R. P., Emami, R., Falcke, H., Farah, J., Fish, V. L., Fomalont, E., Ford, H. A., Fraga-Encinas, R., Freeman, W. T., Friberg, P., Fromm, C. M., Fuentes, A., Galison, P., Gammie, C. F., García, R., Gentaz, O., Georgiev, B., Goddi, C., Gold, R., Gómez-Ruiz, A. I., Gómez, J. L., Gu, M., Gurwell, M., Hada, K., Haggard, D., Haworth, K., Hecht, M. H., Hesper, R., Heumann, D., Ho, L. C., Ho, P., Honma, M., Huang, C.-W. L., Huang, L., Hughes, D. H., Ikeda, S., Impellizzeri, C. M. V., Inoue, M., Issaoun, S., James, D. J., Jannuzi, B. T., Janssen, M., Jeter, B., Jiang, W., Jiménez-Rosales, A., Johnson, M. D., Jorstad, S., Joshi, A. V., Jung, T., Karami, M., Karuppusamy, R., Kawashima, T., Keating, G. K., Kettenis, M., Kim, D.-J., Kim, J.-Y., Kim, J., Kim, J., Kino, M., Koay, J. Y., Kocherlakota, P., Kofuji, Y., Koch, P. M., Koyama, S., Kramer, C., Kramer, M., Krichbaum, T. P., Kuo, C.-Y., La Bella, N., Lauer, T. R., Lee, D., Lee, S.-S., Leung, P. K., Levis, A., Li, Z., Lico, R., Lindahl, G., Lindqvist, M., Lisakov, M., Liu, J., Liu, K., Liuzzo, E., Lo, W.-P., Lobanov, A. P.,

Loinard, L., Lonsdale, C. J., Lu, R.-S., Mao, J., Marchili, N., Markoff, S., Marrone, D. P., Marscher, A. P., Martí-Vidal, I., Matsushita, S., Matthews, L. D., Medeiros, L., Menten, K. M., Michalik, D., Mizuno, I., Mizuno, Y., Moran, J. M., Moriyama, K., Moscibrodzka, M., Müller, C., Mus, A., Musoke, G., Myserlis, I., Nadolski, A., Nagai, H., Nagar, N. M., Nakamura, M., Narayan, R., Narayanan, G., Natarajan, I., Nathanail, A., Navarro Fuentes, S., Neilsen, J., Neri, R., Ni, C., Noutsos, A., Nowak, M. A., Oh, J., Okino, H., Olivares, H., Ortiz-León, G. N., Oyama, T., Özel, F., Palumbo, D. C. M., Paraschos, G. F., Park, J., Parsons, H., Patel, N., Pen, U.-L., Pesce, D. W., Piétu, V., Plambeck, R., PopStefanija, A., Porth, O., Pöttl, F. M., Prather, B., Preciado-López, J. A., Psaltis, D., Pu, H.-Y., Ramakrishnan, V., Rao, R., Rawlings, M. G., Raymond, A. W., Rezzolla, L., Ricarte, A., Ripperda, B., Roelofs, F., Rogers, A., Ros, E., Romero-Cañizales, C., Roshanineshat, A., Rottmann, H., Roy, A. L., Ruiz, I., Ruszczyk, C., Rygl, K. L. J., Sánchez, S., Sánchez-Argüelles, D., Sánchez-Portal, M., Sasada, M., Satopathy, K., Savolainen, T., Schloerb, F. P., Schonfeld, J., Schuster, K.-F., Shao, L., Shen, Z., Small, D., Sohn, B. W., Soohoo, J., Souccar, K., Sun, H., Tazaki, F., Tetarenko, A. J., Tiede, P., Tilanus, R. P. J., Titus, M., Torne, P., Traianou, E., Trent, T., Trippe, S., Turk, M., van Bemmell, I., van Langevelde, H. J., van Rossum, D. R., Vos, J., Wagner, J., Ward-Thompson, D., Wardle, J., Weintroub, J., Wex, N., Wharton, R., Wielgus, M., Wiik, K., Witzel, G., Wondrak, M. F., Wong, G. N., Wu, Q., Yamaguchi, P., Yoon, D., Young, A., Young, K., Younsi, Z., Yuan, F., Yuan, Y.-F., Zensus, J. A., Zhang, S., Zhao, G.-Y., Zhao, S.-S., EHT Collaboration

PUBLICATION: *The Astrophysical Journal*, 930, L14

PUBLICATION DATE: 05/2022

ABSTRACT: <https://ui.adsabs.harvard.edu/abs/2022ApJ...930L..14A>

DOI: 10.3847/2041-8213/ac6429

TITLE: First Sagittarius A* Event Horizon Telescope Results. II. EHT and Multiwavelength Observations, Data Processing, and Calibration

AUTHOR: Akiyama, K., Alberdi, A., Alef, W., Algaba, J. C., Anantua, R., Asada, K., Azulay, R., Bach, U., Baczko, A.-K., Ball, D., Baloković, M., Barrett, J., Bauböck, M., Benson, B. A., Bintley, D., Blackburn, L., Blundell, R., Bouman, K. L., Bower, G. C., Boyce, H., Bremer, M., Brinkerink, C. D., Brissenden, R., Britzen, S., Broderick, A. E., Brogiere, D., Bronzwaer, T., Bustamante, S., Byun, D.-Y., Carlstrom, J. E., Ceccobello, C., Chael, A., Chan, C.-kwan., Chatterjee, K., Chatterjee, S., Chen, M.-T., Chen, Y., Cheng, X., Cho, I., Christian, P., Conroy, N. S., Conway, J. E., Cordes, J. M., Crawford, T. M., Crew, G. B., Cruz-Orsorio, A., Cui, Y., Davelaar, J., De Laurentis, M., Deane, R., Dempsey, J., Desvignes, G., Dexter, J., Dhruv, V., Doleman, S. S., Dougal, S., Dzib, S. A., Eatough, R. P., Emami, R., Falcke, H., Farah, J., Fish, V. L., Fomalont, E., Ford, H. A., Fraga-Encinas, R., Freeman, W. T., Friberg, P., Fromm, C. M., Fuentes, A., Galison, P., Gammie, C. F., García, R., Gentaz, O., Georgiev, B., Goddi, C., Gold, R., Gómez-Ruiz, A. I., Gómez, J. L., Gu, M., Gurwell, M., Hada, K., Haggard, D., Haworth, K., Hecht, M. H., Hesper, R., Heumann, D., Ho, L. C., Ho, P., Honma, M., Huang, C.-W. L., Huang, L., Hughes, D. H., Ikeda, S., Impellizzeri, C. M. V., Inoue, M., Issaoun, S., James, D. J., Jannuzi, B. T., Janssen, M., Jeter, B., Jiang, W., Jiménez-Rosales, A., Johnson, M. D., Jorstad, S., Joshi, A. V., Jung, T., Karami, M., Karuppusamy, R., Kawashima, T., Keating, G. K., Kettenis, M., Kim, D.-J., Kim, J.-Y., Kim, J., Kim, J., Kino, M., Koay, J. Y., Kocherlakota, P., Kofuji, Y., Koch, P. M., Koyama, S., Kramer, C., Kramer, M., Krichbaum, T. P., Kuo, C.-Y., La Bella, N., Lauer, T. R., Lee, D., Lee, S.-S., Leung, P. K., Levis, A., Li, Z., Lico, R., Lindahl, G., Lindqvist, M., Lisakov, M., Liu, J., Liu, K., Liuzzo, E., Lo, W.-P., Lobanov, A. P., Loinard, L., Lonsdale, C. J., Lu, R.-S., Mao, J., Marchili, N., Markoff, S., Marrone, D. P., Marscher, A. P., Martí-Vidal, I., Matsushita, S., Matthews, L. D., Medeiros, L., Menten, K. M., Michalik, D., Mizuno, I., Mizuno, Y., Moran, J. M., Moriyama, K., Moscibrodzka, M., Müller, C., Mus, A., Musoke, G., Myserlis, I., Nadolski, A., Nagai, H., Nagar, N. M., Nakamura, M., Narayan, R., Narayanan, G., Natarajan, I., Nathanail, A., Navarro Fuentes, S., Neilsen, J., Neri, R., Ni, C., Noutsos, A., Nowak, M. A., Oh, J., Okino, H., Olivares, H., Ortiz-León, G. N., Oyama, T., Özel, F., Palumbo, D. C. M., Paraschos, G. F., Park, J., Parsons, H., Patel, N., Pen, U.-L., Pesce, D. W., Piétu, V., Plambeck, R., PopStefanija, A., Porth, O., Pöttl, F. M., Prather, B., Preciado-López, J. A., Psaltis, D., Pu, H.-Y., Ramakrishnan, V., Rao, R., Rawlings, M. G., Raymond, A. W., Rezzolla, L., Ricarte, A., Ripperda, B., Roelofs, F., Rogers, A., Ros, E., Romero-Cañizales, C., Roshanineshat, A., Rottmann, H., Roy, A. L., Ruiz, I., Ruszczyk, C., Rygl, K. L. J., Sánchez, S., Sánchez-Argüelles, D., Sánchez-Portal, M., Sasada, M., Satopathy, K., Savolainen, T., Schloerb, F. P., Schonfeld, J., Schuster, K.-F., Shao, L., Shen, Z., Small, D., Sohn, B. W., Soohoo, J., Souccar, K., Sun, H., Tazaki, F., Tetarenko, A. J., Tiede, P., Tilanus, R. P. J., Titus, M., Torne, P., Traianou, E., Trent, T., Trippe, S., Turk, M., van Bemmell, I., van Langevelde, H. J., van Rossum, D. R., Vos, J., Wagner, J., Ward-Thompson, D., Wardle, J., Weintroub, J., Wex, N., Wharton, R., Wielgus, M., Wiik, K., Witzel, G., Wondrak, M. F., Wong, G. N., Wu, Q., Yamaguchi, P., Yoon, D., Young, A., Young, K., Younsi, Z., Yuan, F., Yuan, Y.-F., Zensus, J. A., Zhang, S., Zhao, G.-Y., Zhao, S.-S., Agurto, C., Araneda, J. P., Arriagada, O., Bertarini, A., Berthold, R., Blanchard, J., Brown, K.,

Cárdenas, M., Cantzler, M., Caro, P., Chuter, T. C., Ciechanowicz, M., Coulson, I. M., Crowley, J., Degenaar, N., Dornbusch, S., Durán, C. A., Forster, K., Geertsema, G., González, E., Graham, D., Gueth, F., Han, C.-C., Herrera, C., Herrero-Illana, R., Heyminck, S., Hoge, J., Huang, Y.-D., Jiang, H., John, D., Klein, T., Kubo, D., Kuroda, J., Kwon, C., Laing, R., Liu, C.-T., Liu, K.-Y., Mac-Auliffe, F., Martin-Cocher, P., Matulonis, C., Messias, H., Meyer-Zhao, Z., Montenegro-Montes, F., Montgomerie, W., Muders, D., Nishioka, H., Norton, T. J., Olivares, R., Pérez-Beaupuits, J. P., Parra, R., Poirier, M., Pradel, N., Raffin, P. A., Ramírez, J., Reynolds, M., Saez-Madain, A. F., Santana, J., Silva, K. M., Sousa, D., Stahm, W., Torstensson, K., Venegas, P., Walther, C., Wieching, G., Wijnands, R., Wouterloot, J. G. A., EHT Collaboration

PUBLICATION: *The Astrophysical Journal*, 930, L13

PUBLICATION DATE: 05/2022

ABSTRACT: <https://ui.adsabs.harvard.edu/abs/2022ApJ...930L..13A>

DOI: 10.3847/2041-8213/ac6675

TITLE: First Sagittarius A* Event Horizon Telescope Results. I. The Shadow of the Supermassive Black Hole in the Center of the Milky Way

AUTHOR: Akiyama, K., Alberdi, A., Alef, W., Algaba, J. C., Anantua, R., Asada, K., Azulay, R., Bach, U., Baczko, A.-K., Ball, D., Baloković, M., Barrett, J., Bauböck, M., Benson, B. A., Bintley, D., Blackburn, L., Blundell, R., Bouman, K. L., Bower, G. C., Boyce, H., Bremer, M., Brinkerink, C. D., Brissenden, R., Britzen, S., Broderick, A. E., Brogiere, D., Bronzwaer, T., Bustamante, S., Byun, D.-Y., Carlstrom, J. E., Ceccobello, C., Chael, A., Chan, C.-kwan., Chatterjee, K., Chatterjee, S., Chen, M.-T., Chen, Y., Cheng, X., Cho, I., Christian, P., Conroy, N. S., Conway, J. E., Cordes, J. M., Crawford, T. M., Crew, G. B., Cruz-Osorio, A., Cui, Y., Davelaar, J., De Laurentis, M., Deane, R., Dempsey, J., Desvignes, G., Dexter, J., Dhruv, V., Doleman, S. S., Dougal, S., Dzib, S. A., Eatough, R. P., Emami, R., Falcke, H., Farah, J., Fish, V. L., Fomalont, E., Ford, H. A., Fraga-Encinas, R., Freeman, W. T., Friberg, P., Fromm, C. M., Fuentes, A., Galison, P., Gammie, C. F., García, R., Gentaz, O., Georgiev, B., Goddi, C., Gold, R., Gómez-Ruiz, A. I., Gómez, J. L., Gu, M., Gurwell, M., Hada, K., Haggard, D., Haworth, K., Hecht, M. H., Hesper, R., Heumann, D., Ho, L. C., Ho, P., Honma, M., Huang, C.-W. L., Huang, L., Hughes, D. H., Ikeda, S., Impellizzeri, C. M. V., Inoue, M., Issaoun, S., James, D. J., Jannuzi, B. T., Janssen, M., Jeter, B., Jiang, W., Jiménez-Rosales, A., Johnson, M. D., Jorstad, S., Joshi, A. V., Jung, T., Karami, M., Karuppusamy, R., Kawashima, T., Keating, G. K., Kettenis, M., Kim, D.-J., Kim, J.-Y., Kim, J., Kim, J., Kino, M., Koay, J. Y., Kocherlakota, P., Kofuji, Y., Koch, P. M., Koyama, S., Kramer, C., Kramer, M., Krichbaum, T. P., Kuo, C.-Y., La Bella, N., Lauer, T. R., Lee, D., Lee, S.-S., Leung, P. K., Levis, A., Li, Z., Lico, R., Lindahl, G., Lindqvist, M., Lisakov, M., Liu, J., Liu, K., Liuzzo, E., Lo, W.-P., Lobanov, A. P., Loinard, L., Lonsdale, C. J., Lu, R.-S., Mao, J., Marchili, N., Markoff, S., Marrone, D. P., Marscher, A. P., Martí-Vidal, I., Matsushita, S., Matthews, L. D., Medeiros, L., Menten, K. M., Michalik, D., Mizuno, I., Mizuno, Y., Moran, J. M., Moriyama, K., Moscibrodzka, M., Müller, C., Mus, A., Musoke, G., Myserlis, I., Nadolski, A., Nagai, H., Nagar, N. M., Nakamura, M., Narayan, R., Narayanan, G., Natarajan, I., Nathanail, A., Navarro Fuentes, S., Neilsen, J., Neri, R., Ni, C., Noutsos, A., Nowak, M. A., Oh, J., Okino, H., Olivares, H., Ortiz-León, G. N., Oyama, T., Özel, F., Palumbo, D. C. M., Paraschos, G. F., Park, J., Parsons, H., Patel, N., Pen, U.-L., Pesce, D. W., Piétu, V., Plambeck, R., PopStefanija, A., Porth, O., Pötzl, F. M., Prather, B., Preciado-López, J. A., Psaltis, D., Pu, H.-Y., Ramakrishnan, V., Rao, R., Rawlings, M. G., Raymond, A. W., Rezzolla, L., Ricarte, A., Ripperda, B., Roelofs, F., Rogers, A., Ros, E., Romero-Cañizales, C., Roshanineshat, A., Rottmann, H., Roy, A. L., Ruiz, I., Ruszczyk, C., Rygl, K. L. J., Sánchez, S., Sánchez-Argüelles, D., Sánchez-Portal, M., Sasada, M., Satpathy, K., Savolainen, T., Schloerb, F. P., Schonfeld, J., Schuster, K.-F., Shao, L., Shen, Z., Small, D., Sohn, B. W., SooHoo, J., Souccar, K., Sun, H., Tazaki, F., Tetarenko, A. J., Tiede, P., Tilanus, R. P. J., Titus, M., Torne, P., Traianou, E., Trent, T., Trippe, S., Türk, M., van Bemmell, I., van Langevelde, H. J., van Rossum, D. R., Vos, J., Wagner, J., Ward-Thompson, D., Wardle, J., Weintroub, J., Wex, N., Wharton, R., Wielgus, M., Wiik, K., Witzel, G., Wondrak, M. F., Wong, G. N., Wu, Q., Yamaguchi, P., Yoon, D., Young, A., Young, K., Younsi, Z., Yuan, F., Yuan, Y.-F., Zensus, J. A., Zhang, S., Zhao, G.-Y., Zhao, S.-S., Agurto, C., Allardi, A., Amestica, R., Araneda, J. P., Arriagada, O., Berghuis, J. L., Bertarini, A., Berthold, R., Blanchard, J., Brown, K., Cárdenas, M., Cantzler, M., Caro, P., Castillo-Domínguez, E., Chan, T. L., Chang, C.-C., Chang, D. O., Chang, S.-H., Chang, S.-C., Chen, C.-C., Chilson, R., Chuter, T. C., Ciechanowicz, M., Colin-Beltran, E., Coulson, I. M., Crowley, J., Degenaar, N., Dornbusch, S., Durán, C. A., Everett, W. B., Faber, A., Forster, K., Fuchs, M. M., Gale, D. M., Geertsema, G., González, E., Graham, D., Gueth, F., Halverson, N. W., Han, C.-C., Han, K.-C., Hasegawa, Y., Hernández-Rebollar, J. L., Herrera, C., Herrero-Illana, R., Heyminck, S., Hirota, A., Hoge, J., Hostler Schimpf, S. R., Howie, R. E., Huang, Y.-D., Jiang, H., Jinchi, H., John, D., Kimura, K., Klein, T., Kubo, D., Kuroda, J., Kwon, C., Lacasse, R., Laing, R., Leitch, E. M., Li, C.-T., Liu, C.-T., Liu, K.-Y., Lin, L. C.-C., Lu, L.-M., Mac-Auliffe, F., Martin-Cocher, P., Matulonis, C., Maute, J. K., Messias, H., Meyer-Zhao, Z., Montaña, A., Montenegro-Montes, F., Montgomerie, W., Moreno Nolasco,

M. E., Muders, D., Nishioka, H., Norton, T. J., Nystrom, G., Ogawa, H., Olivares, R., Oshiro, P., Pérez-Beaupuits, J. P., Parra, R., Phillips, N. M., Poirier, M., Pradel, N., Qiu, R., Raffin, P. A., Rahlin, A. S., Ramírez, J., Ressler, S., Reynolds, M., Rodríguez-Montoya, I., Saez-Madain, A. F., Santana, J., Shaw, P., Shirkey, L. E., Silva, K. M., Snow, W., Sousa, D., Sridharan, T. K., Stahm, W., Stark, A. A., Test, J., Torstensson, K., Venegas, P., Walther, C., Wei, T.-S., White, C., Wieching, G., Wijnands, R., Wouterloot, J. G. A., Yu, C.-Y., Yu, W., Zeballos, M., EHT Collaboration

PUBLICATION: *The Astrophysical Journal*, 930, L12

PUBLICATION DATE: 05/2022

ABSTRACT: <https://ui.adsabs.harvard.edu/abs/2022ApJ...930L..12A>

DOI: 10.3847/2041-8213/ac6674

TITLE: Effects of Magnetic Field Orientations in Dense Cores on Gas Kinematics in Protostellar Envelopes

AUTHOR: Gupta, A., Yen, H.-W., Koch, P., Bastien, P., Bourke, T. L., Chung, E. J., Hasegawa, T., Hull, C. L. H., Inutsuka, S.-. ichiro ., Kwon, J., Kwon, W., Lai, S.-P., Lee, C. W., Lee, C.-F., Pattle, K., Qiu, K., Tahani, M., Tamura, M., Ward-Thompson, D.

PUBLICATION: *The Astrophysical Journal*, 930, 67

PUBLICATION DATE: 05/2022

ABSTRACT: <https://ui.adsabs.harvard.edu/abs/2022ApJ...930...67G>

DOI: 10.3847/1538-4357/ac63bc

TITLE: A BL Lacertae Object at a Cosmic Age of 800 Myr

AUTHOR: Koptelova, E., Hwang, C.-Y.

PUBLICATION: *The Astrophysical Journal*, 929, L7

PUBLICATION DATE: 04/2022

ABSTRACT: <https://ui.adsabs.harvard.edu/abs/2022ApJ...929L...7K>

DOI: 10.3847/2041-8213/ac61e0

TITLE: A SUBLIME 3D Model for Cometary Coma Emission: The Hypervolatile-rich Comet C/2016 R2 (PanSTARRS)

AUTHOR: Cordiner, M. A., Coulson, I. M., Garcia-Berrios, E., Qi, C., Lique, F., Zołtowski, M., de Val-Borro, M., Kuan, Y.-J., Ip, W.-H., Mairs, S., Roth, N. X., Charnley, S. B., Milam, S. N., Tseng, W.-L., Chuang, Y.-L.

PUBLICATION: *The Astrophysical Journal*, 929, 38

PUBLICATION DATE: 04/2022

ABSTRACT: <https://ui.adsabs.harvard.edu/abs/2022ApJ...929...38C>

DOI: 10.3847/1538-4357/ac5893

TITLE: Virial Clumps in Central Molecular Zone Clouds

AUTHOR: Myers, P. C., Hatchfield, H. P., Battersby, C.

PUBLICATION: *The Astrophysical Journal*, 929, 34

PUBLICATION DATE: 04/2022

ABSTRACT: <https://ui.adsabs.harvard.edu/abs/2022ApJ...929...34M>

DOI: 10.3847/1538-4357/ac5906

TITLE: Multiwavelength Analysis and the C IV $\lambda 1549$ Å Emission Line Behavior From 2008 to 2020 of FSRQ B2 1633+382

AUTHOR: Amaya-Almazán, R. A., Chavushyan, V., Patiño-Álvarez, V. M.

PUBLICATION: *The Astrophysical Journal*, 929, 14

PUBLICATION DATE: 04/2022

ABSTRACT: <https://ui.adsabs.harvard.edu/abs/2022ApJ...929...14A>

DOI: 10.3847/1538-4357/ac5741

TITLE: Connecting Galactic and extragalactic outflows: From the Cygnus-X cluster to active galaxies
AUTHOR: Skretas, I. M., Kristensen, L. E.
PUBLICATION: *Astronomy and Astrophysics*, 660, A39
PUBLICATION DATE: 04/2022
ABSTRACT: <https://ui.adsabs.harvard.edu/abs/2022A&A...660A..39S>
DOI: 10.1051/0004-6361/202141944

TITLE: The Nature of 500 Micron Risers II: Sub-mm Faint Dusty Star Forming Galaxies
AUTHOR: Cairns, J., Clements, D. L., Greenslade, J., Petitpas, G., Cheng, T., Ding, Y., Parmar, A., Pérez-Fournon, I., Riechers, D.
PUBLICATION: *arXiv e-prints*, arXiv:2203.01049
PUBLICATION DATE: 03/2022
ABSTRACT: <https://ui.adsabs.harvard.edu/abs/2022arXiv220301049C>

TITLE: Evolution and Kinematics of Protostellar Envelopes in the Perseus Molecular Cloud
AUTHOR: Heimsoth, D. J., Stephens, I. W., Arce, H. G., Bourke, T. L., Myers, P. C., Dunham, M. M.
PUBLICATION: *The Astrophysical Journal*, 927, 88
PUBLICATION DATE: 03/2022
ABSTRACT: <https://ui.adsabs.harvard.edu/abs/2022ApJ...927...88H>
DOI: 10.3847/1538-4357/ac448e

TITLE: New Tests of Milli-lensing in the Blazar PKS 1413 + 135
AUTHOR: Peirson, A. L., Liodakis, I., Readhead, A. C. S., Lister, M. L., Perlman, E. S., Aller, M. F., Blandford, R. D., Grainge, K. J. B., Green, D. A., Gurwell, M. A., Hodges, M. W., Hovatta, T., Kiehlmann, S., Lähteenmäki, A., Max-Moerbeck, W., Mcaloon, T., O'Neill, S., Pavlidou, V., Pearson, T. J., Ravi, V., Reeves, R. A., Scott, P. F., Taylor, G. B., Titterton, D. J., Tornikoski, M., Vedantham, H. K., Wilkinson, P. N., Williams, D. T., Zensus, J. A.
PUBLICATION: *The Astrophysical Journal*, 927, 24
PUBLICATION DATE: 03/2022
ABSTRACT: <https://ui.adsabs.harvard.edu/abs/2022ApJ...927...24P>
DOI: 10.3847/1538-4357/ac469e

TITLE: A search for cool molecular gas in GK Persei and other classical novae
AUTHOR: Kamiński, T., Mazurek, H. J., Menten, K. M., Tyłenda, R.
PUBLICATION: *Astronomy and Astrophysics*, 659, A109
PUBLICATION DATE: 03/2022
ABSTRACT: <https://ui.adsabs.harvard.edu/abs/2022A&A...659A.109K>
DOI: 10.1051/0004-6361/202142737

TITLE: Unlocking the sulphur chemistry in intermediate-mass protostars of Cygnus X. Connecting the cold and warm chemistry
AUTHOR: el Akel, M., Kristensen, L. E., Le Gal, R., van der Walt, S. J., Pitts, R. L., Dulieu, F.
PUBLICATION: *Astronomy and Astrophysics*, 659, A100
PUBLICATION DATE: 03/2022
ABSTRACT: <https://ui.adsabs.harvard.edu/abs/2022A&A...659A.100E>
DOI: 10.1051/0004-6361/202141810

TITLE: Detection of HC180+ in a Protoplanetary Disk: Exploring Oxygen Isotope Fractionation of CO
AUTHOR: Furuya, K., Tsukagoshi, T., Qi, C., Nomura, H., Cleaves, L. I., Lee, S., Yoshida, T. C.
PUBLICATION: *The Astrophysical Journal*, 926, 148
PUBLICATION DATE: 02/2022
ABSTRACT: <https://ui.adsabs.harvard.edu/abs/2022ApJ...926..148F>
DOI: 10.3847/1538-4357/ac45ff

TITLE: A Multitransition Methanol Maser Study of the Accretion Burst Source G358.93-0.03-MM1
AUTHOR: Bayandina, O. S., Brogan, C. L., Burns, R. A., Chen, X., Hunter, T. R., Kurtz, S. E., MacLeod, G. C., Sobolev, A. M., Sugiyama, K., Valts, I. E., Yonekura, Y.
PUBLICATION: *The Astronomical Journal*, 163, 83
PUBLICATION DATE: 02/2022
ABSTRACT: <https://ui.adsabs.harvard.edu/abs/2022AJ....163...83B>
DOI: 10.3847/1538-3881/ac42d2



The Submillimeter Array (SMA) is a pioneering radio-interferometer dedicated to a broad range of astronomical studies including finding protostellar disks and outflows; evolved stars; the Galactic Center and AGN; normal and luminous galaxies; and the solar system. Located on Maunakea, Hawaii, the SMA is a collaboration between the Smithsonian Astrophysical Observatory and the Academia Sinica Institute of Astronomy and Astrophysics.

SUBMILLIMETER ARRAY
Center for Astrophysics | Harvard & Smithsonian
60 Garden Street, MS 78
Cambridge, MA 02138 USA
www.cfa.harvard.edu/sma/

SMA HILO OFFICE
645 North A'ohoku Place
Hilo, Hawaii 96720
Ph. 808.961.2920
Fx. 808.961.2921
sma1.sma.hawaii.edu

ACADEMIA SINICA INSTITUTE
OF ASTRONOMY & ASTROPHYSICS
11F of Astronomy-Mathematics Building,
AS/NTU, No. 1, Sec. 4, Roosevelt Road
Taipei 10617
Taiwan R.O.C.
www.asiaa.sinica.edu.tw/